Cosmological matter perturbations

Jiun-Huei Proty Wu
Astronomy Department, University of California, Berkeley,
601 Campbell Hall, Berkeley, CA 94720-3411, USA

We investigate matter density perturbations in models of structure formation with or without causal/acausal source. Under the fluid approximation in the linear theory, we first derive full perturbation equations in flat space with a cosmological constant Λ. We then use Green-function technique to obtain analytic solutions for matter perturbations in a flat $\Lambda = 0$ model. Some incorrect solutions in the literature are corrected here. A simple yet accurate extrapolation scheme is then proposed to obtain solutions in curved or $\Lambda \neq 0$ cosmologies. Some general features of these solutions are revealed. In particular, we analytically prove that the resulting matter density perturbations are independent of the way the causal source was compensated into the background contents of the universe when it was first formed. We also use our Green-function solutions to investigate the compensation mechanism for perturbations with causal seeds, and yield a mathematically and physically explicit form in interpreting it. We found that the compensation scale depends not only on the dynamics of the universe, but also on the properties of the seeds near the horizon scale. It can be accurately located by employing our Green functions.

I. INTRODUCTION

The standard cosmology was lack of a mechanism to produce cosmological perturbations. In order to compensate for this flaw in the standard model, there are currently two main paradigms for structure formation—inflation [1] and topological defects [2]. While the beauty and simplicity of the former appears to have enticed more adherents and studies, the latter has proved computationally much more challenging to make robust predictions with which to confront observations [3–12]. These two paradigms are fundamentally different in the way they generate cosmological perturbations. The standard adiabatic inflation produces primordial perturbations on all scales of cosmological interest via quantum fluctuations and the causal constraint during inflation, and these perturbations grow over time in an uncorrelated manner. As a consequence, the perturbations today can be thought of as simply transfered from the initial irregularities that inflation set up, and this transfer function can be easily obtained in the linear theory and thus well understood in the literature. On the other hand, topological defects are the byproducts of the spontaneous symmetry-breaking phase transition in the early universe, and hence carry energy that was carved out of the originally homogeneous background energy of the universe. Therefore due to causality, defects induce perturbations only on sub-horizon scales, via gravitational interactions while evolving. This mechanism that prevents the growth of super-horizon perturbations is called the 'compensation mechanism'. In addition, due to the certain topology of the defect network, the resulting perturbations are correlated and thus non-Gaussian, in contrast to the standard adiabatic inflationary perturbations. It then follows that to compute the perturbations in models with defects, we need to know the evolution history of defects for the entire dynamic range during which the cosmological perturbations of our interest were seeded. This is what makes the computation of defect-induced perturbations so difficult.

In the literature the power spectra of this kind of models have been investigated using the full Einstein-Boltzmann equations. However, the study of the phase information of these perturbations still remains difficult because of the limited computation power. Although there have been some detailed treatments for theories with causal seeds [14,15], we shall in this paper present a simpler formalism, which is an approximation to the full Einstein-Boltzmann equations, to provide not only a physically transparent way for understanding the evolution of density perturbations in models with source, but also a computationally economical scheme to investigate the phase information of the resulting cosmological perturbations. This formalism is parallel to those presented in Ref. [16] and Ref. [17], but we give some modifications to incorporate the inclusion of the cosmological constant and a more detailed treatment for the effect of baryon-photon coupling/decoupling. We also note that part of the solutions in Ref. [16] are incorrect due to the incorrect initial conditions and the incorrect assumptions about the form of the subsequent perturbations induced by the source (see text later). We shall correct these mistakes and further provide a complete and explicit set of analytic solutions for the matter density perturbations. With an accurate extrapolation scheme, these solutions become also valid for models with any reasonably chosen background cosmology. The formalism and its solutions to be developed here will be completely general and thus suitable for any models with or without causal/acausal source.

The structure of this paper is as follows. In section II, under the fluid approximation, we first derive in the synchronous gauge the full perturbation equations with source terms, in flat cosmologies with a cosmological constant Λ. This is done by considering the stress-energy conservation of the fluids (IIA) and the source (IIB), and the linearly perturbed Einstein equations (IIC). The fluid components considered here are cold dark matter (CDM), baryons (B), and photons (γ), and we employ the baryon-photon tight-coupling approximation to derive the perturbation equations before the last-scattering epoch. In this context, we also investigate the role of the so-called stress-energy pseudotensor (IID). The initial conditions of these perturbation equations are discussed (IIE), and we use the approximation of instantaneous decoupling to deal with the decoupling of photons and baryons at the epoch of last scattering (IIF). We then numerically justify the accuracy of this formalism in the context of standard CDM models, by comparing its results with those of the full Einstein-Boltzmann solver [13] (IIG). Within reasonable ranges of cosmological parameters, our approach provides satisfactory precision at greatly reduced numerical cost.

In section III, we derive the matter perturbation solutions of the equations presented in section II. The perturbations of radiation and matter are first divided into two parts: the initial and the subsequent perturbations. With some change of variables, these equations are then ready to be solved by the Green-function technique (IIIA). With this technique, we find the exact solutions on scales much larger or much smaller than the horizon size, namely the super-horizon or the sub-horizon solutions respectively (IIIB). Some degeneracy among the Green functions for the matter perturbation solutions is then found and used to reduce their effective number (IIIC). With this great simplification, solutions on intermediate scales are then easily obtained by an accurate interpolation scheme based on the well-known standard CDM transfer function (IIID). We also discuss the effect of baryons (IIIE). A simple and accurate extrapolation scheme is then introduced to obtain solutions in the $K \neq 0$ or $\Lambda \neq 0$ cosmologies (IIIF), where K is the curvature of the universe (see Appendix A). All our Green-function solutions are numerically verified to high accuracy.

In section IV, we use our Green-function solutions to investigate some important properties of cosmological matter density perturbations. We first demonstrate the relation between our solutions and the standard CDM transfer function (IV A). We also prove that in models with causal source, the resulting matter perturbations today are independent of the way the source energy is initially compensated into the background contents of the universe (IV B). Finally we use our Green-function solutions to study the compensation mechanism and the scale on which it operates (IV C). We find that this compensation scale is determined not only by the dynamics of the universe, but also by the properties of the source near the horizon scale. Once the detailed features of the source near the horizon scale are known, this compensation scale can be accurately located using our Green functions. A summary and conclusion is given in section V. In appendix A, we define the convention of some notations used in this paper, and present for reference the solutions for the dynamics of various background cosmologies, including the consideration of non-zero curvature and a cosmological constant.

II. SYNCHRONOUS GAUGE PERTURBATION THEORY

In this section, we derive the linear evolution equations for cosmological perturbations. To calculate the density and metric perturbations, we model the contents of the universe as perfect fluids: radiation (photons and neutrinos) and pressureless matter (CDM and baryons). We shall use the photon-baryon tight-coupling approximation until the epoch of last scattering, at which we assume instantaneous decoupling, also taking into account the effect of Silk damping due to the photon diffusion. After the decoupling, the baryonic perturbations originating from the perturbations of the photon-baryon coupled fluid are then merged linearly into the CDM content. In scenarios with causal seeds, the radiation and matter fields are assumed to be initially uniform, and then perturbed by the causal seeds after they are formed. The radiation, matter, and causal seeds are assumed to interact only through gravity, meaning that their stress-energy tensors are separately covariantly conserved.

We shall work in the synchronous gauge, in which the perturbations $h_{\mu\nu}$ to the spacetime metric $g_{\mu\nu}$ obey the constraint $h_{0\mu} = 0$. Throughout this paper, we use a signature $(-+++)$ for the spacetime metric, and units in which $\hbar = c = k_B = 1$. Thus the perturbed flat Friedmann-Robertson-Walker (FRW) metric is given by

$$g_{00} = -a^2(\tau); \quad g_{ij} = a^2(\tau)[\delta_{ij} + h_{ij}(\tau;\mathbf{x})]: \tag{2.1}$$

We shall work in the linear theory, requiring $|h_{ij}| \ll 1$. Greek alphabet will denote the spacetime indices (e.g. $\mu = 0;1;2;3$), and mid-alphabet Latin letters the spatial indices (e.g. $i = 1;2;3$). Although the synchronous gauge is sometimes criticised in the literature due to its residual gauge freedom, it is still well suited to models in which the universe evolves from being perfectly homogeneous and isotropic. In such models, all perturbation variables can be initially set to zero (before the causal seeds are generated), and this is normally referred to as the 'initially unperturbed synchronous gauge' (IUSG) [16]. It possesses no residual gauge freedom. Thus the Einstein equations are completely causal in IUSG, with the values of all perturbation variables at a given spacetime point being completely determined by initial conditions within the past light cone of the point. One example of such models is the cosmic defect models, which have been of most interest in the study of models with causal seeds.

In section IIA, we derive in the IUSG the conservation equations of radiation and matter fields. In section IIB, we consider the conservation of source stress energy. In section IIC, we derive the linearly perturbed Einstein equations. Then, in section IID, we employ the concept of stress-energy pseudotensor to investigate the internal energy transfer among various fields. In section IIF, we describe the approximation of instantaneous decoupling of photons and baryons at the epoch of last scattering. In section IIG, we numerically verify the accuracy of our formalism for the standard CDM model, in comparison with the results from CMBFAST [13], a fast Einstein-Boltzmann solver.

A. Stress-energy conservation of radiation and matter fields

The contents of the universe are considered as perfect fluids, whose energy-momentum tensors have the form

$$T^{\mu}_{N\nu} = (\rho_N + p_N) u^{\mu}_N u_{N\nu} + p_N \delta^{\mu}_{\nu}; \quad \text{with } u^{\mu}_N u_{N\mu} = -1. \tag{2.2}$$

Here ρ_N, p_N, and u^{μ}_N are the density, pressure, and four-velocity of the Nth fluid respectively. In the homogeneous background, we have $u^{\mu}_N = (a^{-1}; \vec{0})$, which implies that $\delta u^{0}_N = 0$ to first order. We thus define the velocity perturbation as $v^{i}_N = a\,\delta u^{i}_N$, i.e., $\delta u^{\mu}_N = (0; \vec{v}_N/a)$. The equation of state and the sound speed are defined respectively as

$$w_N = \frac{p_N}{\rho_N}; \quad c^2_N = \frac{\dot{p}_N}{\dot{\rho}_N}. \tag{2.3}$$

Consequently, the covariant conservation of stress energy for each fluid $T^{\mu}_{N\nu;\mu} = 0$ gives [16]

$$\dot{\delta}_N + (1 + w_N)\left(\nabla\cdot\vec{v}_N + \frac{1}{2}\dot{h}\right) + 3\frac{\dot{a}}{a}(c^2_N - w_N)\delta_N = 0; \tag{2.4}$$

$$\dot{\vec{v}}_N + \frac{\dot{a}}{a}(1 - 3c^2_N)\vec{v}_N + \frac{c^2_N}{1 + w_N}\nabla\delta_N = 0; \tag{2.5}$$

$$\dot{\vec{v}}^{\perp}_N + \frac{\dot{a}}{a}(1 - 3c^2_N)\vec{v}^{\perp}_N = 0; \tag{2.6}$$

where $\delta_N = \delta\rho_N/\rho_N$, $h \equiv h_{ii}$ is the spatial trace of h_{ij}, and we have decomposed the velocities as $\vec{v}_N = \vec{v}^{\parallel}_N + \vec{v}^{\perp}_N$, with $\nabla\times\vec{v}^{\parallel}_N = 0$ and $\nabla\cdot\vec{v}^{\perp}_N = 0$.

In the regime of photon-baryon tight coupling, we have only two main fluids: the CDM component and the tightly-coupled photon-baryon fluid. They will be denoted as $N = c; B$ respectively, and discussed separately as follows. Note that we have ignored the neutrinos in the radiation.

1. CDM fluid

We first consider the CDM fluid, i.e. $N = c$. With $w_c = c^2_c = 0$ for pressureless matter, the equations of stress-energy conservation (2.4)–(2.6) become

$$\dot{\delta}_c + \nabla\cdot\vec{v}_c = -\frac{1}{2}\dot{h}; \quad \dot{\vec{v}}_c + \frac{\dot{a}}{a}\vec{v}_c = 0. \tag{2.7}$$

As we can see, any perturbations in the CDM velocity will decay as a^{-1}. Thus we can simply choose $\vec{v}_c = \vec{0}$ in the IUSG. Once $\vec{v}_c = \vec{0}$, it will remain so as there is no linear gravitational source. As a consequence, the CDM obeys a single nontrivial conservation law resulting from equation (2.7)

$$\dot{h} + 2\dot{\delta}_c = 0 \Rightarrow h = -2\delta_c, \tag{2.8}$$

where the second equation results from the initial condition $h = \delta_c = 0$, as required by the IUSG.

2. Photon-baryon tightly coupled fluid and its photon component

For the tightly-coupled photon-baryon (γB) fluid, we have

$$v_{\gamma B} = v_\gamma = v_B; \quad p_{\gamma B} = p_\gamma; \quad \rho_{\gamma B} = \rho_\gamma + \rho_B: \tag{2.9}$$

Thus we can define

$$R = \frac{\dot\rho_B}{\dot\rho_\gamma} = \frac{3\rho_B}{4\rho_\gamma}; \tag{2.10}$$

where the second result comes from the fact that $\rho_\gamma \propto a^{-4}$ and $\rho_B \propto a^{-3}$. Definitions (2.3) then give

$$w_{\gamma B} = \frac{1}{3+4R}; \quad c^2_{\gamma B} = \frac{1}{3(1+R)}: \tag{2.11}$$

With these results, the equations of stress-energy conservation for the γB fluid can be obtained from equations (2.4)–(2.6):

$$\dot\delta_{\gamma B} + \frac{4+4R}{3+4R}(\nabla\cdot v_{\gamma B} - \dot\delta_c) + \frac{\dot a}{a}\frac{R}{(1+R)(3+4R)}\delta_{\gamma B} = 0; \tag{2.12}$$

$$\dot v_{\gamma B} + \frac{\dot a}{a}\frac{R}{1+R}v_{\gamma B} + \frac{3+4R}{12(1+R)^2}\nabla\delta_{\gamma B} = 0; \tag{2.13}$$

$$\dot v^{\perp}_{\gamma B} + \frac{\dot a}{a}\frac{R}{1+R}v^{\perp}_{\gamma B} = 0: \tag{2.14}$$

In cosmological applications, such as CMB anisotropies, we are more interested in the photon perturbations rather than the perturbations in the γB fluid. Therefore by using equations (2.9) and (2.10), we can extract the photon component from the above equations to yield [18]

$$\dot\delta_r + \frac{4}{3}\nabla\cdot v_r - \frac{4}{3}\dot\delta_c = 0; \tag{2.15}$$

$$\dot v_r + \frac{\dot a}{a}\frac{R}{1+R}v_r + \frac{1}{4+4R}\nabla\delta_r = 0; \tag{2.16}$$

where we have ignored neutrinos in the radiation so as to replace the subscript γ with r. The velocity can then be eliminated to yield a single second-order equation:

$$\ddot\delta_r - \frac{4}{3}\ddot\delta_c + \frac{\dot R}{1+R}\left(\dot\delta_r - \frac{4}{3}\dot\delta_c\right) - \frac{1}{3+3R}\nabla^2\delta_r = 0: \tag{2.17}$$

We note that although the photon velocities are missing in this equation, they can be recovered at any given moment using equation (2.15).

An alternative presentation of equations (2.15) and (2.17) is via the entropy perturbation s. It is defined as the fluctuation in the number of photons per dark matter particle

$$s = \frac{3}{4}\delta_r - \delta_c: \tag{2.18}$$

Thus equations (2.15) and (2.17) can be rewritten as

$$\dot s = -\nabla\cdot v_r \tag{2.19}$$

$$\ddot s = -\frac{\dot R}{1+R}\dot s + \frac{1}{3+3R}\nabla^2(s+\delta_c): \tag{2.20}$$

As we shall see, δ_r can only have a white noise power spectrum on super-horizon scales. From equation (2.16), this implies a k^2 power spectrum in v_r on these scales. Adding the fact that the entropy fluctuation s starts from zero on super-horizon scales due to the fixed number of dark matter particles per photon, it then follows from equation (2.19) that both s and $\dot s$ have a k^4 falloff outside the horizon. Therefore in numerical simulations, as long as the initial horizon size is smaller than the scales of our interest, we can simply set $s = \dot s = 0$ as part of the initial condition.

B. Stress-energy conservation of the source

The causal source we shall consider is weak, so it will appear only as first-order terms in the perturbed Einstein equations. Thus in the linear theory we are considering here, they can be treated as being stiff, meaning that their evolution depends only on their own self-interactions and the background dynamics of the universe, but not on their self-gravity or on the weak gravitational field of the inhomogeneities they produce. This assumption will enable us to separate the calculation of their dynamics from that of the inhomogeneities they induce, allowing us to evolve them as if they are in a completely homogeneous background. Since the source is stiff, its energy-momentum tensor need only be locally covariantly conserved with respect to the background:

$$\Theta_{00;0} + \frac{\dot a}{a}\Theta_+ = -\Theta_{0i;i}\,; \tag{2.21}$$

$$\Theta_{0i;0} + 2\frac{\dot a}{a}\Theta_{0i} = -\Theta_{ij;j}\,; \tag{2.22}$$

where $\Theta_+ = \Theta_{00} + \Theta_{ii}$.

Another important aspect of cosmic structure formation with causal seeds like cosmic defects is the fact that the sources, formed at very early times, will ultimately create under-densities in the initially homogeneous background, out of which they are carved. This is a direct result of energy conservation in the universe, and is normally termed 'compensation'. We shall discuss this issue in more detail later.

C. Linearly Perturbed Einstein equations

At first we have ten Einstein equations

$$R_{\mu\nu} = 8\pi G\left(T_{\mu\nu} - \frac{1}{2}g_{\mu\nu}T\right) + \Lambda g_{\mu\nu}\,; \tag{2.23}$$

or equivalently,

$$G_{\mu\nu} \equiv R_{\mu\nu} - \frac{1}{2}g_{\mu\nu}R_S = 8\pi G T_{\mu\nu} - \Lambda g_{\mu\nu}\,; \tag{2.24}$$

where $R_{\mu\nu}$ is the Ricci tensor, G is the gravitational constant, $T = g^{\mu\nu}T_{\mu\nu}$, Λ is the cosmological constant, $G_{\mu\nu}$ is the Einstein tensor, and $R_S \equiv g^{\mu\nu}R_{\mu\nu}$ is the scalar curvature. Linearly perturbing the above equations, we obtain

$$\delta R_{\mu\nu} = 8\pi G\left(\delta T_{\mu\nu} - \frac{1}{2}h_{\mu\nu}\eta^{rs}T_{rs} - \frac{1}{2}\eta_{\mu\nu}\eta^{rs}\delta T_{rs} + \frac{1}{2}\eta_{\mu\nu}h_{pq}\eta^{rp}\eta^{sq}T_{rs}\right) + a^2\Lambda h_{\mu\nu}\,; \tag{2.25}$$

or equivalently,

$$\delta G_{\mu\nu} = 8\pi G\,\delta T_{\mu\nu} - a^2\Lambda h_{\mu\nu}\,; \tag{2.26}$$

where

$$\delta T_{\mu\nu} = \Theta_{\mu\nu} + a^2\sum_N \left(h_{\mu r}T^r_{N\nu} + \eta_{\mu s}\,\delta T^s_{N\nu}\right). \tag{2.27}$$

A closed set of the ten linearly perturbed Einstein equations are then

$$2\delta R_{00} = -\ddot h - \frac{\dot a}{a}\dot h = +3\left(\frac{\dot a}{a}\right)^2\sum_N \left(1 + 3c_N^2\right)\Omega_N\delta_N + 8\pi G\Theta_+\,; \tag{2.28}$$

$$2\left\{\delta\tilde R_{ij} - \left[\frac{\ddot a}{a} + \left(\frac{\dot a}{a}\right)^2\right]\tilde h_{ij}\right\} = \ddot{\tilde h}_{ij} + 2\frac{\dot a}{a}\dot{\tilde h}_{ij} - \nabla^2\tilde h_{ij} - \frac{1}{3}h_{;ij} + \frac{1}{9}\delta_{ij}\nabla^2 h$$
$$+\tilde h_{ik;kj} + \tilde h_{jk;ki} - \frac{2}{3}\delta_{ij}\tilde h_{kl;kl} = 16\pi G\,\tilde\Theta_{ij} + a^2\Lambda\tilde h_{ij}\,; \tag{2.29}$$

$$2\delta G_{00} = \tilde h_{ij;ij} - \frac{2}{3}\nabla^2 h + 2\frac{\dot a}{a}\dot h = 6\left(\frac{\dot a}{a}\right)^2\sum_N \Omega_N\delta_N + 16\pi G\Theta_{00}\,; \tag{2.30}$$

$$2\delta G_{0i} = \dot{\tilde h}_{ij;j} - \frac{2}{3}\dot h_{;i} = -6\left(\frac{\dot a}{a}\right)^2\sum_N (1 + w_N)\Omega_N v_N^i + 16\pi G\Theta_{0i}\,; \tag{2.31}$$

where the traceless parts are defined by $\tilde R_{ij} = R_{ij} - \delta_{ij}R^k{}_k/3$, and similarly for $\tilde h_{ij}$ and $\tilde\Theta_{ij}$. The prime over the sum in equation (2.31) indicates the sum over all fluids except CDM. We note from the above results that in the IUSG the cosmological constant Λ does not appear as extra terms in the perturbation equations except in (2.29), the 'ij' component.

Within the photon-baryon tight-coupling regime, the above perturbation equations simplify as:

$$\ddot h - \frac{\dot a}{a}\dot h = +3\left(\frac{\dot a}{a}\right)^2[(2+R)\Omega_r\delta_r + \Omega_c\delta_c] + 8\pi G\Theta_+ ; \tag{2.32}$$

$$\ddot{\tilde h}_{ij} + 2\frac{\dot a}{a}\dot{\tilde h}_{ij} - \nabla^2\tilde h_{ij} - \frac13 h_{;ij} + \frac19\delta_{ij}\nabla^2 h + \tilde h_{ik;kj} + \tilde h_{jk;ki} - \frac23\delta_{ij}\tilde h_{kl;kl} = 16\pi G\tilde\Theta_{ij} + a^2\Lambda\tilde h_{ij} ; \tag{2.33}$$

$$\tilde h_{ij;ij} - \frac23\nabla^2 h + 2\frac{\dot a}{a}\dot h = -6\left(\frac{\dot a}{a}\right)^2[\Omega_c\delta_c + (1+R)\Omega_r\delta_r] + 16\pi G\Theta_{00} ; \tag{2.34}$$

$$\dot{\tilde h}_{ij;j} - \frac23\dot h_{;i} = -8\left(\frac{\dot a}{a}\right)^2(1+R)\Omega_r v_r^i + 16\pi G\Theta_{0i} : \tag{2.35}$$

We note that if the source obeys the covariant conservation equations (2.21) and (2.22), then equations (2.34) and (2.35) are preserved by equations (2.32).

In the standard CDM model where the source is absent, equation (2.32) can be greatly simplified on super-horizon scales ($k\tau \ll 1$) in the radiation or matter era:

$$\ddot\delta_c + \frac1\tau\dot\delta_c - \frac{2(2+R)}{\tau^2}\delta_c = 0;\ \text{in radiation era,} \tag{2.36}$$

$$\ddot\delta_c + \frac2\tau\dot\delta_c - \frac{6}{\tau^2}\delta_c = 0;\ \text{in matter era:} \tag{2.37}$$

Since $R = 3\Omega_{B0}a/4\Omega_{c0}a_{eq}$ by definition, we know $R \ll 1$ deep in the radiation era. Thus the above equations both have a growing mode $\delta_c \propto \tau^2$. This result has an important implication for numerical simulations of structure formation with causal sources. In this case, if numerical errors appear as white noise on super-horizon modes $k < 1/\tau$, then they will have a growing behavior $S(k) = 4\pi k^3 P(k) \propto k^3\tau^4$. For the horizon crossing mode $k \sim 1/\tau$, this becomes $S(k) \propto \tau$ [17]. This means that although energy conservation together with causality should forbid the growth of perturbations on super-horizon scales, any numerical errors seeded from early times would induce a spurious growing mode on these scales. To overcome this problem, one needs to perfectly compensate the source energy in the initially homogeneous background. In the following section, we shall discuss one of the methods that can achieve this.

D. Stress-energy conservation of the pseudotensor

The concept of the stress-energy pseudotensor in an expanding universe was first remarked in this context by Veeraraghavan and Stebbins [16], and further investigated by Pen, Spergel and Turok [17]. To introduce this concept, we start from a perturbed Minkowski space $\hat g_{\mu\nu} = \eta_{\mu\nu} + \hat h_{\mu\nu}$, where the Bianchi identity $\nabla^\mu G_{\mu\nu} = 0$ leads to an ordinary conservation law $\partial^\mu G_{\mu\nu}^{(1)} = 0$ at linear order in $\hat h_{\mu\nu}$. Adding the fact that the Einstein equations give $G_{\mu\nu}^{(1)} = 8\pi G T_{\mu\nu} - G_{\mu\nu}^{(nl)}$ where $G_{\mu\nu}^{(nl)}$ is the sum of non-linear terms in $\hat h_{\mu\nu}$, we see that the right-hand side of this equation provides an ordinarily conserved tensor, the stress-energy pseudotensor.

The generalization of this result to an FRW model is straightforward, with only the corrections due to the expansion of the universe. Moving all these corrections (derivatives of the scale factor) to the right-hand side of the Einstein equations while keeping only the linear terms in $h_{\mu\nu}$, we obtain a pseudo-stress-energy tensor $\tau_{\mu\nu} \equiv G_{\mu\nu}^{(1)}/8\pi G$:

$$\tau_{00} = \frac{3}{8\pi G}\left(\frac{\dot a}{a}\right)^2[\Omega_c\delta_c + (1+R)\Omega_r\delta_r] - \frac{1}{8\pi G}\frac{\dot a}{a}\dot h + \Theta_{00} ; \tag{2.38}$$

$$\tau_{0i} = -\frac{1}{2\pi G}\left(\frac{\dot a}{a}\right)^2(1+R)\Omega_r v_r^i + \Theta_{0i} ; \tag{2.39}$$

$$\tau_{ij} = \delta_{ij}\frac{1}{8\pi G}\left(\frac{\dot a}{a}\right)^2\Omega_r\delta_r - \frac{1}{8\pi G}\frac{\dot a}{a}\left(\dot{\tilde h}_{ij} - \frac23\dot h\delta_{ij}\right) + \Theta_{ij} : \tag{2.40}$$

This tensor obeys an ordinary conservation law $\tau_{\mu\nu;\nu} = 0$ according to the Einstein equations, or equivalently

$$\tau^{00}_{;0} = -\tau^{0i}_{;i}\,; \tag{2.41}$$

$$\tau^{i0}_{;0} = -\tau^{ij}_{;j}\,: \tag{2.42}$$

This is not a fundamentally new conservation law, but it describes the interchange of energy and momentum among the different components in the universe, i.e. the radiation, matter, and the source in our case. This description appears to be physically more transparent than the original Einstein equations.

Another advantage of invoking this formalism is that it is easier for numerical simulations to specify the initial conditions and to maintain proper compensation on super-horizon scales. As we shall explain later, τ_{ij} can only have a white-noise power spectrum on super-horizon scales. Thus integrating equations (2.41) and (2.42) over time shows that τ_{00} has a k^4 power spectrum and that τ_{0i} has a k^2 power spectrum. Therefore, as long as the horizon size at the beginning of the simulation is smaller than the scales of our interest, we can set $\tau_{00} = \tau_{0i} = 0$ as the initial condition, allowing for perturbations to grow only inside the horizon and for τ_{00} to fall off as k^4 outside the horizon. For simulations of structure formation with causal source, a check of $\tau_{00} \propto k^4$ on super-horizon modes will tell us whether or not the compensation is well obeyed.

To make use of the pseudo-stress-energy tensor formalism in the study of cosmological perturbations, we combine the conservation equation for radiation (2.20), the definition of pseudoenergy (2.38), and one of the alternative Einstein equations using the pseudo-stress-energy tensor (2.41), to yield a convenient closed set of equations:

$$\ddot{s} = -\frac{\dot{R}}{1+R}\dot{s} + \frac{1}{3+3R}\nabla^2(s+\delta_c)\,; \tag{2.43}$$

$$\ddot{\delta}_c = 4\pi G\frac{a}{\dot{a}}(\tau_{00} - \Theta_{00}) - \frac{\dot{a}}{a}\left[\frac{3}{2}\delta_c + 2(1+R)\,\delta_r - \delta_c + 2(1+R)\,\delta_r s\right]; \tag{2.44}$$

$$\dot{\tau}_{00} = -\tau_{0i,i} + \frac{1}{2\pi G}\left(\frac{\dot{a}}{a}\right)^2 (1+R)\,\delta_r \dot{s}\,: \tag{2.45}$$

Here we have used equations (2.8), (2.18), (2.19) and (2.39) to eliminate $\dot{h}$, δ_r, v_r^i and τ_{0i} respectively. By analogy to the results in Ref. [17], here we have built both the pseudoenergy τ_{00} and the entropy fluctuation s into the above formalism.

E. Initial conditions of causal models

As required by the IUSG, all perturbation variables are zero before any mechanism of structure formation starts to act on the initially homogeneous and isotropic universe. In causal models, causality also requires that local physical processes can never induce correlated perturbations on scales much larger than the horizon. Therefore, when the initial irregularities of the universe are first formed (e.g. via the formation of cosmic defects, or the presence of inflation), the spatial part of $\Theta_{\mu\nu}$, δ, and h can only have white-noise power spectra on super-horizon modes — their spatial perturbations being uncorrelated on scales larger than the horizon size [16]. The same applies to δ_N and therefore h. It then follows from equations (2.16), (2.22) and (2.42) respectively that the power spectra of v_r, Θ_{0i} and τ_{0i} all fall off as k^2 outside the horizon. From equations (2.19) and (2.41), we also have the spectra of s, $\dot{s}$ and τ_{00} proportional to k^4 on these scales, as previously discussed. As a summary, we have for super-horizon modes $k\tau \ll 1$ that

$$\delta_c;\ \delta_r; h; h_{ij};\ \Theta_{ij};\ \tau_{ij} \propto k^0\,; \tag{2.46}$$

$$v_r;\ \Theta_{0i};\ \tau_{0i} \propto k^1\,; \tag{2.47}$$

$$s; \dot{s};\ \tau_{00} \propto k^2\,; \tag{2.48}$$

where '$\propto k^n$' means the power spectrum is proportional to k^{2n}.

Since the production time of the initial irregularities is normally so early that the horizon size τ_i at that time is much smaller than the cosmological scales k_{cos}^{-1} of our interest (i.e. $k_{cos}\tau_i \ll 1$), the above conditions can be regarded as general initial conditions for all scales of cosmological interest. If we require $k_{cos}\tau_i \ll 1$ in our analysis, we can simply choose

$$v_r^i = \Theta_{0i} = \tau_{0i} = s = \dot{s} = \tau_{00} = 0; \tag{2.49}$$

as the initial conditions, because their power spectra all decay as either k^2 or k^4 outside the horizon.

With such a choice, we can see from equation (2.38) that there is still freedom for the choice of δ_c, δ_r and $\hbar$ into which to compensate ρ_{00} when ρ_{00} was first formed. Nevertheless, as we shall analytically prove later, no matter how ρ_{00} was compensated into the background contents of the universe when the causal source was first formed, the resulting matter density perturbations today would be the same. We note that this was first numerically observed in Ref. [17], and here we shall provide a thorough interpretation to it using our analytical solutions to be obtained later. We also note that none of the above arguments will hold if the initial perturbations are seeded in an acausal way, which is nevertheless not of our current interest.

F. approximation of instantaneous decoupling

One thing we have not included in our formalism is the treatment at and after the decoupling epoch η_d. Before this epoch, photons and baryons are assumed to be tightly coupled, forming a single γB fluid. At the decoupling epoch η_d, baryons and photons are assumed to be instantaneously decoupled from each other, so that δ_γ and δ_B evolve separately afterwards. A numerical fit to the redshift of the decoupling epoch is [19]

$$z_d = 1291\frac{(\Omega_{m0}h^2)^{0.251}}{1+0.659(\Omega_{m0}h^2)^{0.828}}\left[1+b_1(\Omega_{B0}h^2)^{b_2}\right]; \tag{2.50}$$

$$b_1 = 0.313(\Omega_{m0}h^2)^{-0.419}\left[1+0.607(\Omega_{m0}h^2)^{0.674}\right]; \tag{2.51}$$

$$b_2 = 0.238(\Omega_{m0}h^2)^{0.223}. \tag{2.52}$$

Although this is the result for the decoupling epoch of baryons and there is another fit for that of photons, these two epochs—the recombination of baryons and the last scattering of photons—coincide approximately in the absence of subsequent reionization [20,21].

In addition, the photons and baryons are not in fact perfectly coupled, and this leads to the diffusion damping of photons and Silk damping of baryons [22] during the decoupling epoch. To model these effects, we apply damping envelopes to both δ_γ and δ_B at the decoupling epoch z_d, i.e.

$$\hat{\delta}_{N(d)} = \tilde{\delta}_{N(d)}D_N(k); \quad N = \gamma, B; \tag{2.53}$$

where the tilde indicates the Fourier transform of a quantity and k is the wave number. The photon diffusion damping envelope can be approximated by the form [21]

$$D_\gamma(k) \simeq e^{-(k/k_\gamma)^{m_\gamma}}; \tag{2.54}$$

where

$$\frac{k_\gamma}{\mathrm{Mpc}^{-1}} = \left\{\frac{2}{\pi}\arctan\left[\frac{\pi}{2}\left(\frac{F_2}{F_1}\right)^{p_2/p_1}(\Omega_{B0}h^2)^{p_2}\right]\right\}^{p_1/p_2}F_1; \tag{2.55}$$

$$m_\gamma = 1.46(\Omega_{m0}h^2)^{0.0303}\left[1+0.128\arctan\left(\ln(32.8\,\Omega_{B0}h^2)^{-0.643}\right)\right]; \tag{2.56}$$

$$p_1 = 0.29; \tag{2.57}$$

$$p_2 = 2.38(\Omega_{m0}h^2)^{0.184}; \tag{2.58}$$

$$F_1 = 0.293(\Omega_{m0}h^2)^{0.545}\left[1+(25.1\,\Omega_{m0}h^2)^{-0.648}\right]; \tag{2.59}$$

$$F_2 = 0.524(\Omega_{m0}h^2)^{0.505}\left[1+(10.5\,\Omega_{m0}h^2)^{-0.564}\right]. \tag{2.60}$$

Silk damping for the baryons can likewise be approximated as [21]

$$D_B(k) \simeq e^{-(k/k_S)^{m_S}}; \tag{2.61}$$

where

$$\frac{k_S}{\mathrm{Mpc}^{-1}} = 1.38(\Omega_{m0}h^2)^{0.398}(\Omega_{B0}h^2)^{0.487}\frac{1+(96.2\,\Omega_{m0}h^2)^{-0.684}}{1+(346\,\Omega_{B0}h^2)^{-0.842}}; \tag{2.62}$$

$$m_S = 1.40\frac{(\Omega_{B0}h^2)^{-0.0297}(\Omega_{m0}h^2)^{0.0282}}{1+(781\,\Omega_{B0}h^2)^{-0.926}}. \tag{2.63}$$

In some scenarios with causal sources, the damping envelopes (2.54) and (2.61) may depart from the form of exponential fall-off here to a power-law decay towards smaller scales. This is due to the survival of perturbations which are actively seeded during the decoupling process. For example, in models with cosmic strings, the departure appears on scales smaller than of order a few arc-minutes (i.e. the multipole index $l \gtrsim 3000$) [23]. Certainly this is beyond the scale range of our interest. Moreover, since the decoupling process is relatively a short instant in the entire evolution history of the perturbations, the contribution from these survived small-scale perturbations should be relatively small. Adding the fact that we expect the post-decoupling contribution in the perturbations seeded by defects to have a power-law fall-off on small scales due to a certain topology of the source [5], the small-scale power in the final perturbations is likely to be dominated by this post-decoupling contribution, rather than the primary perturbations (those seeded before and during the decoupling, whose power spectrum first exponentially decays and then turns to a power-law fall-off). Therefore, on the scales of our interest, the damping approximation employed here should be still appropriate for models with cosmic defects.

Now we consider the evolution of δ_c and δ_B after the decoupling epoch z_d. From the energy conservation law (2.4)–(2.6), we have for the baryon perturbations

$$\ddot{\delta}_B - \ddot{\delta}_c + \frac{\dot{a}}{a}(\dot{\delta}_B - \dot{\delta}_c) = 0: \tag{2.64}$$

This implies $(\dot{\delta}_B - \dot{\delta}_c) \propto a^{-1}$, meaning that the evolution of δ_B and δ_c will soon converge to the same behavior. We also know that matter perturbations grow as τ^2 in the matter era so that $[\delta_{B(d)} - \delta_{c(d)}]$ is relatively small when compared with either δ_{B0} or δ_{c0}. As a consequence, in the calculation of δ_{B0} and δ_{c0} to linear order, it is appropriate to combine δ_B and δ_c at the decoupling epoch z_d as

$$\tilde{\delta}_{m(d)} = \frac{\Omega_{B0}\hat{\delta}_{B(d)} + \Omega_{c0}\tilde{\delta}_{c(d)}}{\Omega_{B0} + \Omega_{c0}} = \frac{3\Omega_{B0}\tilde{\delta}_{\gamma(d)}D_B/4 + \Omega_{c0}\tilde{\delta}_{c(d)}}{\Omega_{B0} + \Omega_{c0}}; \tag{2.65}$$

and the same for their time derivatives. Then we have only two fluids after the decoupling: the photon fluid (γ) and the matter fluid, which is linearly combined from the CDM and baryon fluids ($\Omega_m = \Omega_c + \Omega_B$). Eventually we can take the matter perturbations at the present epoch to be $\tilde{\delta}_{c0} \simeq \tilde{\delta}_{B0} \simeq \tilde{\delta}_{m0}$.

To sum up, we first evolve the CDM and γB perturbations up to the decoupling epoch z_d given by (2.50), noting that our formalism extracts the photon component γ from the γB fluid. We then apply damping envelopes to $\tilde{\delta}_{\gamma(d)}$ and $\tilde{\delta}_{c(d)}$, as illustrated by equation (2.53), to account for the photon diffusion and Silk damping. $\tilde{\delta}_{m(d)}$ is then obtained by linearly combining $\tilde{\delta}_{c(d)}$ and $\tilde{\delta}_{B(d)}$, as shown in equation (2.65). Finally we carry on the evolution of $\tilde{\delta}_m$ and $\tilde{\delta}_r$ from the epoch z_d to the present, using our previous perturbation equations with $R = 0$ and the subscript 'c' replaced by 'm'.

G. Accuracy for the standard CDM models

To verify our scheme for evolving cosmological perturbations, we first calculate the CDM transfer function in the context of the adiabatic inflationary CDM model:

$$T_c(k;\tau_0) = \frac{\tilde{\delta}_c(k;\tau_0)\tilde{\delta}_c(0;0)}{\tilde{\delta}_c(k;0)\tilde{\delta}_c(0;\tau_0)}; \tag{2.66}$$

where τ_0 is the present conformal time. To this end, we employ equations (2.43), (2.44) and (2.45) in the absence of the source terms, and the approximation of instantaneous decoupling described above. We start the evolution in the deep radiation era when $\Omega_m/\Omega_r \ll 1$, $R \ll 1$, and $\tau_i \ll 1/k$ for a given mode k. In this case, one choice of the initial conditions is

$$s = \dot{s} = 0; \quad \delta_c = \tau_i^2; \quad \phi_{00} = \frac{1}{G}: \tag{2.67}$$

Figure 1 shows our results for the CDM transfer functions $T_c(k;\tau_0)$ at the present epoch in different cosmologies, together with the results obtained from CMBFAST [13]. It is clear that they agree very well. The discrepancy of the two reaches its maximum of about 5% at the scale $k \sim 1hMpc^{-1}$ in the open model with $\Omega_{c0} = 0.15$ and $\Omega_{B0} = 0.05$. We have also checked our results against those in Ref. [24], and they are in agreement again within a 5% error. In

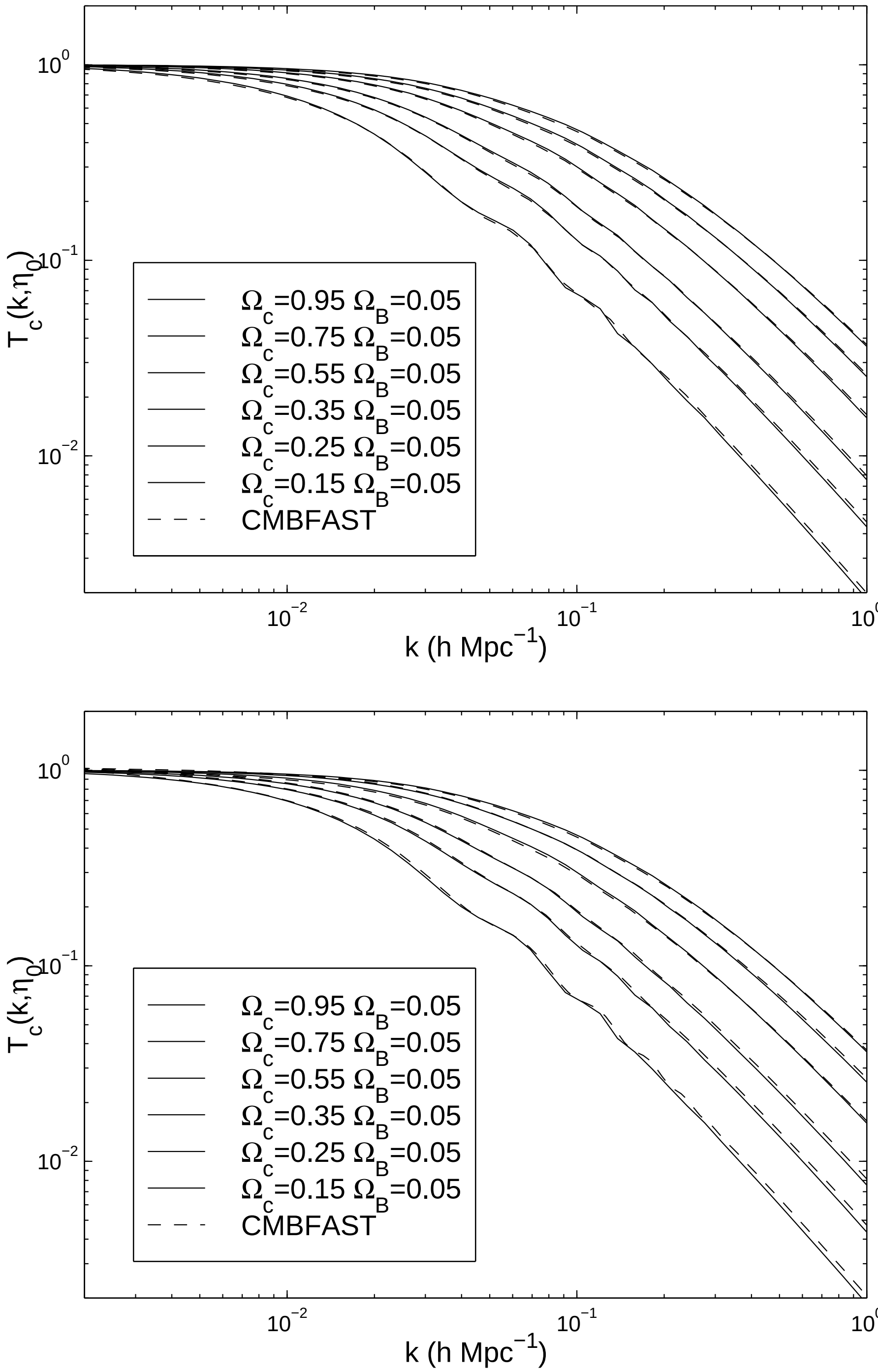

FIG. 1. Comparison of our CDM transfer functions at the present epoch $T_c(k;\eta_0)$ with results obtained from CMBFAST [13]. On the top are results in flat models with a cosmological constant (i.e. $\Omega_{\Lambda 0} + \Omega_{c0} + \Omega_{B0} = 1$). At the bottom are results in open models without a cosmological constant. Results using our formalism are plotted as solid lines, while the results from CMBFAST are plotted as dashed lines. We have used $h = 0.7$ throughout. The mass fraction of Helium-4 $Y_{He} = 0.24$ and the number of neutrino species $N_\nu = 3.04$ have been used in obtaining the results from CMBFAST.

addition, from the bottom curves in Figure 1, we notice the oscillations resulting from the photon-baryon coupling before τ_d in cosmologies with high baryon fractions Ω_{B0}/Ω_{m0}.

Next, we calculate the radiation transfer function at the decoupling epoch, since the radiation perturbations at this epoch will appear as the intrinsic CMB anisotropies. We define this transfer function as:

$$T_r(k;\tau_d) = \frac{\tilde{\delta}_r(k;\tau_d)\tilde{\delta}_c(0;0)}{\tilde{\delta}_c(k;0)\tilde{\delta}_c(0;\tau_0)}; \tag{2.68}$$

where we normalize the radiation perturbations at τ_d to both the amplitude of the super-horizon CDM perturbations today and the initial CDM power spectrum, as we did for $T_c(k;\tau_0)$ (see eq. [2.66]). This definition will enable us to verify not only the scale dependence of the evolution of perturbations, but also their normalizations. Figure 2 shows our results, again as a comparison with the results from CMBFAST. We see that although the scale dependence of our results is slightly different from that of the CMBFAST results, the overall normalisation appears to be quite accurate. The sideway shift of the oscillatory peaks in our results when compared with the peaks from CMBFAST has a maximum of about 5% in the flat model with $\Omega_{c0} = 0.95$ and $\Omega_{B0} = 0.05$. This discrepancy results naturally from the instantaneous-decoupling approximation in our formalism. As a result, despite the small inaccuracy, our formalism provides a much more numerically efficient way than the full Einstein-Boltzmann scheme in calculating the density perturbations.

III. SOLUTIONS OF MATTER PERTURBATIONS

A. Decomposition of perturbations

We first consider density perturbations about a flat FRW model with a cosmological constant Λ, which are causally sourced by an evolving source field with the energy-momentum tensor $\Theta_{\mu\nu}(x;\tau)$. As seen in the previous section, with the photon-baryon tight coupling approximation in the synchronous gauge, the linear evolution equations of the radiation and CDM perturbations can be given by equations (2.43), (2.44) and (2.45), which are derived from equations (2.20), (2.38) and (2.41). This set of equations has the advantage in controling the initial condition for numerical simulations, as well as understanding the law of stress-energy conservation. For analytic simplicity, however, we shall drop the use of Θ_{00} in this section, and employ equations (2.17) and (2.32) to form an alternative set of evolution equations for density perturbations:

$$\ddot{\delta}_r - \frac{4}{3}\ddot{\delta}_c + \frac{\dot{R}}{1+R}\left(\dot{\delta}_r - \frac{4}{3}\dot{\delta}_c\right) - \frac{1}{3(1+R)}\nabla^2\delta_r = 0; \tag{3.1}$$

$$\ddot{\delta}_c + \frac{\dot{a}}{a}\dot{\delta}_c - \frac{3}{2}\left(\frac{\dot{a}}{a}\right)^2\left[\Omega_c\delta_c + (2+R)\Omega_r\delta_r\right] = 4\pi G\Theta_+. \tag{3.2}$$

We note again that the cosmological constant Λ affects only the background dynamics (i.e., the evolution of the scale factor a), but does not contribute extra terms in the above perturbation equations. After the decoupling epoch τ_d, the treatment is essentially the same as that introduced in section IIF. We have numerical verified in the context of the adiabatic inflationary CDM model that the set of equations (3.1) and (3.2) and the set of equations (2.43), (2.44) and (2.45) indeed give identical transfer functions of density perturbations, with a numerical discrepancy of less than 0.1%.

Assuming that the causal source was formed at some initial time τ_i and then evolved to the current time τ, it proves useful to split the source-seeded linear perturbations into initial (I) and subsequent (S) parts [16]:

$$\delta_N(x;\tau) = \delta^I_N(x;\tau) + \delta^S_N(x;\tau); \quad N = c, r. \tag{3.3}$$

The initial perturbations $\delta^I_N(x;\tau)$ originate from the source configuration at τ_i, while the subsequent perturbations $\delta^S_N(x;\tau)$ are actively and cumulatively seeded by the later evolution of the source at each $\hat{\tau}$, where $\tau_i < \hat{\tau} < \tau$. This is equivalent to having the initial conditions

$$\delta^I_N(\tau_i) = \delta_N(\tau_i); \quad \dot{\delta}^I_N(\tau_i) = \dot{\delta}_N(\tau_i); \tag{3.4}$$

$$\delta^S_N(\tau_i) = \dot{\delta}^S_N(\tau_i) = 0. \tag{3.5}$$

Because the source induces isocurvature perturbations, $\delta^I(x;\tau)$ must compensate $\delta^S(x;\tau)$ on comoving scales $|x - x'| > \tau$ to prevent acausal perturbation growth on super-horizon scales. One of the aims of this paper is to show analytically

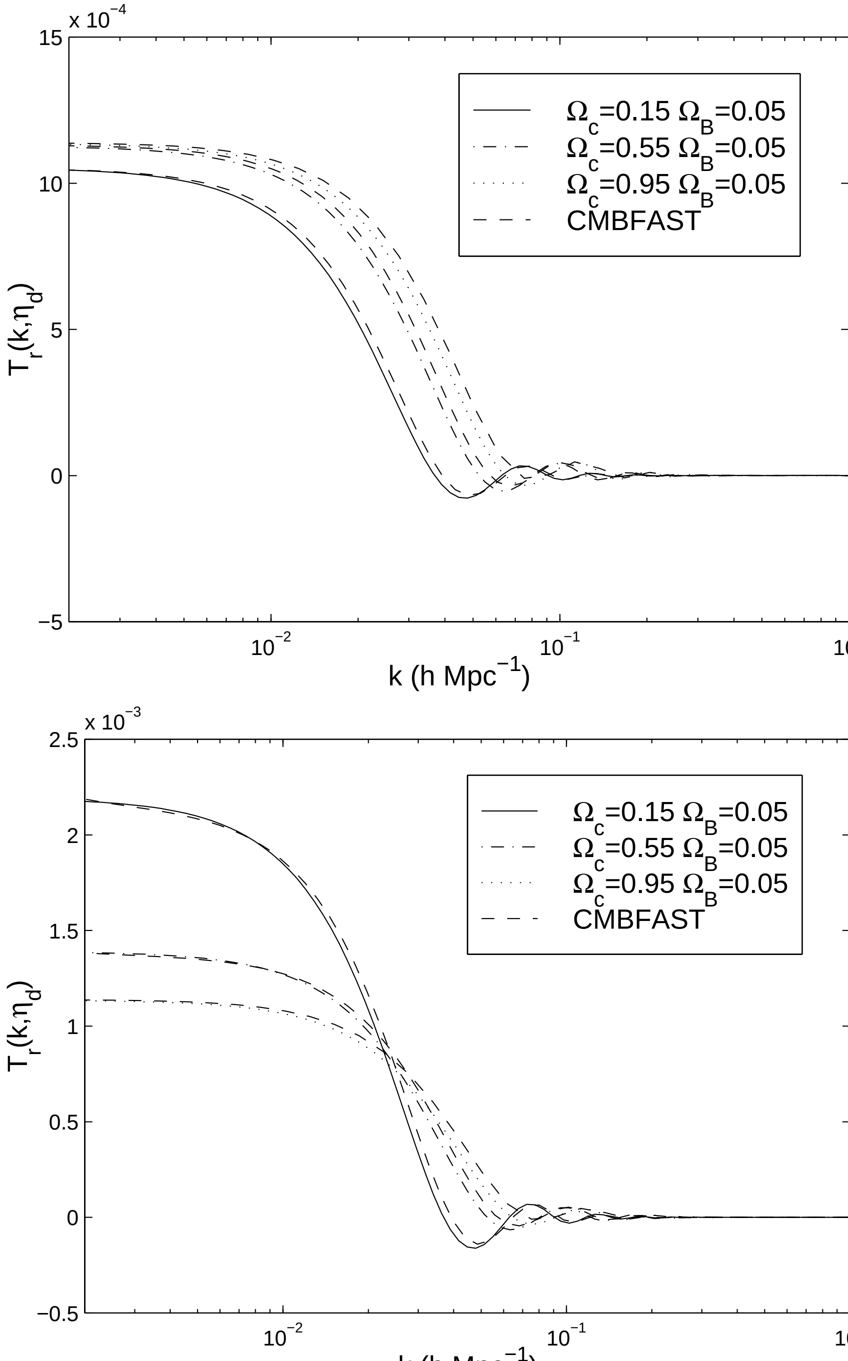

FIG. 2. Comparison of our radiation transfer functions at the decoupling epoch $T_r(k;\eta_d)$ with results obtained from CMBFAST [13]. On the top are results in flat models with a cosmological constant (i.e. $\Omega_{\Lambda 0} + \Omega_{c0} + \Omega_{B0} = 1$). At the bottom are results in open models without a cosmological constant. Our results are plotted as solid, dot-dashed, and dotted lines, while the CMBFAST results are plotted as dashed lines. Note that this transfer function has been normalised to both the amplitude of the super-horizon CDM perturbations today and the initial CDM power spectrum (see eq. [2.68]).

how this compensation mechanism can be achieved. Now we can solve the system of equations (3.1) and (3.2) by employing the integral equation with Green functions:

$$\delta^I_N(x;\tau) = \sum_{N'}\int d^3x' G_1^{NN'}(X;\tau;\tau_i)\,\delta_{N'}(x';\tau_i) + \int d^3x' G_2^{NN'}(X;\tau;\tau_i)\,\dot{\delta}_{N'}(x';\tau_i); \tag{3.6}$$

$$\delta^S_N(x;\tau) = 4\pi G\int_{\tau_i} d\hat{\tau}\int d^3x' G^{Ns}(X;\tau;\hat{\tau})\,\sigma_+(x';\hat{\tau}); \tag{3.7}$$

where $X = |x - x'|$. The easiest method of obtaining the Green-function solutions is to go to Fourier space and solve the resulting homogeneous system of ordinary differential equations with appropriate initial conditions. Since the Green functions depend only on the modulus of $X = |x - x'|$, it follows that their Fourier amplitudes must depend only on the modulus of k. Thus we have

$$\tilde{\delta}^I_N(k;\tau) = \sum_{N'}\left[\tilde{G}_1^{NN'}(k;\tau;\tau_i)\,\tilde{\delta}_{N'}(k;\tau_i) + \tilde{G}_2^{NN'}(k;\tau;\tau_i)\,\dot{\tilde{\delta}}_{N'}(k;\tau_i)\right]; \tag{3.8}$$

$$\tilde{\delta}^S_N(k;\tau) = 4\pi G\int_{\tau_i}^{\tau}\tilde{G}^{Ns}(k;\tau;\hat{\tau})\,\tilde{\sigma}_+(k;\hat{\tau})\,d\hat{\tau}. \tag{3.9}$$

We notice that equation (3.9) is different from the form in Ref. [16], where the authors identified our $\tilde{G}^{Ns}$ as $\tilde{G}_2^{Nc}$. This identification is incorrect, because $\tilde{G}^{Ns}$ and $\tilde{G}_2^{Nc}$ have different initial conditions, as we shall see.

For simplicity, we assume no baryons and therefore set $R = 0$ for now, and shall relax this constraint later. With the change of variable $y = 1 + A\tau/2$ where $A = 2(\sqrt{2}-1)/\tau_{eq}$ (leading to $a/a_{eq} = y^2 - 1$), and with the formalism (3.8) and (3.9), we can rewrite equations (3.1) and (3.2) in Fourier space as

$$\tilde{G}^{r''} - \frac{4}{3}\tilde{G}^{c''} + \frac{4k^2}{3A^2}\tilde{G}^r = 0; \tag{3.10}$$

$$(1-y^2)\tilde{G}^{c''} - 2y\tilde{G}^{c'} + 6 - \frac{12\tilde{G}^r/\tilde{G}^c}{1-y^2}\,\tilde{G}^c = 0; \tag{3.11}$$

where a prime represents a derivative with respect to y, $\tilde{G}^c \equiv \tilde{G}_1^{cN}$, $\tilde{G}_2^{cN}$ or $\tilde{G}^{cs}$, and $\tilde{G}^r \equiv \tilde{G}_1^{rN}$, $\tilde{G}_2^{rN}$ or $\tilde{G}^{rs}$. According to equations (3.8) and (3.9), the initial conditions (3.4) and (3.5) now become:

$$\tilde{G}_1^{cc} = \dot{\tilde{G}}_2^{cc} = \tilde{G}_1^{rr} = \dot{\tilde{G}}_2^{rr} = 1 \quad \text{at} \quad \tau = \tau_i; \tag{3.12}$$

$$\dot{\tilde{G}}^{cs} = \frac{3}{4}\dot{\tilde{G}}^{rs} = 1 \quad \text{at} \quad \tau = \hat{\tau}; \tag{3.13}$$

with all the other Green functions and their time derivatives vanishing. There are three things we should notice here. First, it is required that $\tilde{G}_i^{NN'}(k;\tau;\tau_i) = 0$ for $\tau \le \tau_i$, and that $\tilde{G}^{Ns}(k;\tau;\hat{\tau}) = 0$ for $\tau \le \hat{\tau}$. Second, the Green functions $\tilde{G}_i^{NN'}$ only describe the time dependence of the homogeneous version of equations (3.1) and (3.2), while the Green functions $\tilde{G}^{Ns}$ are, by the conventional definition, the true Green functions used to solve the inhomogeneous equations (3.1) and (3.2). Finally, since there are only four variables in equations (3.10) and (3.11) (i.e. $\tilde{G}^c$, $\tilde{G}^r$, $\dot{\tilde{G}}^c$ and $\dot{\tilde{G}}^r$), there must exist some dependence among the five sets of Green functions (i.e. $\tilde{G}_1^{Nc}$, $\tilde{G}_1^{Nr}$, $\tilde{G}_2^{Nc}$, $\tilde{G}_2^{Nr}$ and $\tilde{G}^{Ns}$). This dependence can be observed from the initial conditions (3.12) and (3.13), which yield

$$\tilde{G}^{Ns} = \tilde{G}_2^{Nc} + \frac{4}{3}\tilde{G}_2^{Nr}. \tag{3.14}$$

In Ref. [16], the authors ignored the fact that $\dot{\tilde{G}}^{rs} = 4/3$ in the initial condition (3.13). This ignorance led to the absence of the second term in equation (3.14) (and thus the identification of $\tilde{G}^{Ns} = \tilde{G}_2^{Nc}$), and consequently the incorrect solutions of Green functions in their final results. Based on equations (3.10) and (3.11) with the initial conditions (3.12) and (3.13), in the following subsections we shall analytically derive a complete set of Green-function solutions for the matter perturbations, which will then be numerically verified.

B. Super-horizon and sub-horizon modes

Under the limit $k \ll 1$ or $k \gg 1$, the ratio $\tilde{G}^r/\tilde{G}^c$ will approach a constant (see below), so that equation (3.11) becomes the associated Legendre equation, with solutions composed of the associated Legendre functions $P_2^{\nu}(y)$ and $Q_2^{\nu}(y)$, where $\nu = \sqrt{12\tilde{G}^r/\tilde{G}^c}$. We shall use subscripts 1 and 0 to denote solutions in the limits $k \gg 1$ and $k \ll 1$ respectively. For simplicity, we shall denote both $\hat{\eta}$ and η_i as $\hat{\eta}$ in the following solutions.

1. $k \gg 1$: When the wavelengths are much smaller than the horizon size, the radiation oscillates many times per expansion time and its effect is therefore negligible. By setting $\tilde{G}^r/\tilde{G}^c = 0$, equation (3.11) can be solved as

$$\tilde{G}_1^c(\eta;\hat{\eta}) = E(\hat{\eta})P_2^0(y) + F(\hat{\eta})Q_2^0(y); \tag{3.15}$$

   where $E(\hat{\eta})$ and $F(\hat{\eta})$ are functions of $\hat{\eta}$. This gives the sub-horizon solutions.

2. $k \ll 1$: When the wavelengths are much longer than the horizon size, we have $\tilde{G}^r/\tilde{G}^c = 4/3$ as the consequence of zero entropy (see eqs. [2.18] and [2.49]), giving $\nu = 4$. Thus equations (3.10) and (3.11) yield

$$\tilde{G}_0^r(\eta;\hat{\eta}) = \frac{4}{3}\tilde{G}_0^c(\eta;\hat{\eta}) + \alpha_i(\eta - \hat{\eta}) + \beta_i; \tag{3.16}$$

$$\begin{aligned}\tilde{G}_0^c(\eta;\hat{\eta}) &= G(\hat{\eta})P_2^{-4}(y) + H(\hat{\eta})Q_2^4(y)\\ &+ 12\int_{y_i}^{y}\frac{Q_2^4(x)P_2^{-4}(y) - P_2^{-4}(x)Q_2^4(y)}{Q_2^4(x)P_2^{-4\prime}(x) - P_2^{-4}(x)Q_2^{4\prime}(x)}\,\frac{A\beta_i + 2\alpha_i(x - y_i)}{A(x^2-1)^2}\,dx;\end{aligned} \tag{3.17}$$

   where α_i and β_i are constants, and $G(\hat{\eta})$ and $H(\hat{\eta})$ are functions of $\hat{\eta}$, all determined by the initial conditions. These are the super-horizon solutions.

Combined with the initial conditions (3.12) and (3.13), equations (3.15) and (3.17) can be solved to yield the following results. For clarity, we shall denote $\hat{y} = 1 + A\hat{\eta}/2$ in $\tilde{G}^{NS}$ and $y_i = 1 + A\eta_i/2$ in $\tilde{G}_i^{NN'}$ both as w:

$$\tilde{G}_1^{cs} = \frac{1}{4A}\left[(w^2-1)\left((3w^2-1)(3y^2-1)\log\frac{(w+1)(y-1)}{(w-1)(y+1)} - 6(y-w)(3wy+1)\right)\right]; \tag{3.18}$$

$$\tilde{G}_0^{cs} = \frac{2(y^6w - w^6y - 5y^4w + 5w^4y + 15y^2w - 15yw^2 + 5w - 5y)}{5A(y^2-1)^2(w^2-1)}; \tag{3.19}$$

$$\begin{aligned}\tilde{G}_{11}^{cc} &= \frac{1}{2}(3y^2-1)(3w^2-2) - \frac{9}{2}wy(w^2-1)\\ &+ \frac{3}{4}w(w^2-1)(3y^2-1)\log\frac{(y+1)(w-1)}{(y-1)(w+1)};\end{aligned} \tag{3.20}$$

$$\tilde{G}_{10}^{cc} = \frac{2yw^5 - 20yw^3 + 20y^2w^2 + 20w^2 - 30yw - 15y^4 - 5 + 3y^6 + 25y^2}{5(y^2-1)^2(w^2-1)}; \tag{3.21}$$

$$\tilde{G}_{21}^{cc} = \tilde{G}_1^{cs}; \tag{3.22}$$

$$\tilde{G}_{20}^{cc} = \tilde{G}_0^{cs} - \frac{4}{3}\tilde{G}_{20}^{cr}; \tag{3.23}$$

$$\tilde{G}_{11}^{cr} = 0; \tag{3.24}$$

$$\tilde{G}_{10}^{cr} = \frac{3(y^6 - 5y^2w^4 + 4yw^5 + 10y^2w^2 - 5y^4 - 5w^4 + 10y^2 - 20yw + 10w^2)}{5(y^2-1)^2(w^2-1)^2}; \tag{3.25}$$

$$\tilde{G}_{21}^{cr} = 0; \tag{3.26}$$

$$\begin{aligned}\tilde{G}_{20}^{cr} &= \frac{3}{10A}\left[\frac{(y^2+4y+5)(y-1)^2}{(y+1)^2}\log\frac{y-1}{w-1} + \frac{(y^2-4y+5)(y+1)^2}{(y+1)^2}\log\frac{w+1}{y+1}\right.\\ &\left.+ 2(w-y)\frac{(4yw^3 - 6y^2w^2 - 10w^2 + y^5w - 4y^2w + 7yw + 6y^2 - 4y^3 + 5 + y^4)}{(w^2-1)(y^2-1)^2}\right].\end{aligned} \tag{3.27}$$

We note that equations (3.22), (3.23) and (3.26) result directly from the initial conditions (3.12) and (3.13). They are consistent with equation (3.14).

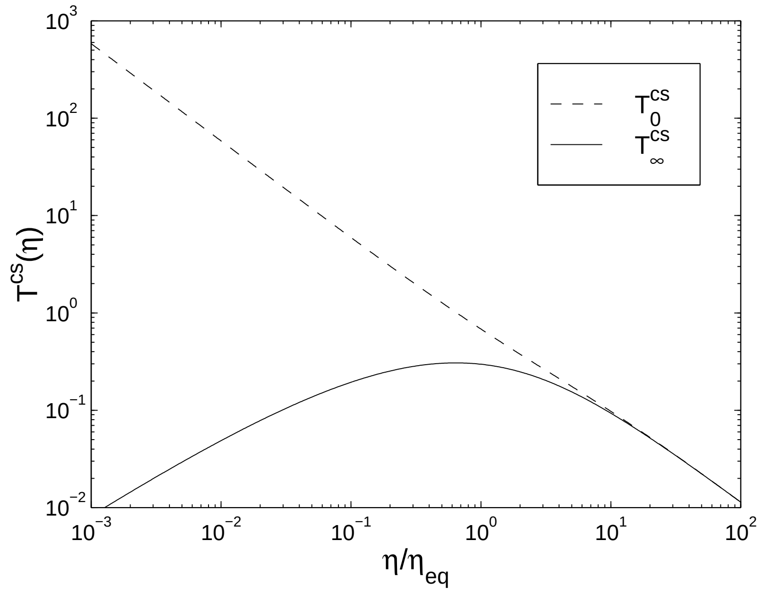

FIG. 3. The source transfer functions $\tilde{T}^{cs}_0$ ($k\eta \ll 1$, dashed line) and $\tilde{T}^{cs}_\infty$ ($k\eta \gg 1$, solid line).

Despite the complicated forms presented here, all these Green functions have simple asymptotic behaviors in the radiation- or matter-dominated regimes. Since we are more interested in the matter perturbations today and we know from equation (3.11) that $\tilde{G}^c \propto \eta^2 \propto a$ when $\eta/\eta_{eq} \to \infty$, we can design a 'source transfer function' as

$$\tilde{T}^{c}(k;\hat\eta) \equiv \lim_{\eta/\eta_{eq}\to\infty} \frac{a_{eq}}{a}\tilde{G}^{c}(k;\eta;\hat\eta) : \tag{3.28}$$

Note that this is different from the definition of the standard CDM transfer function (2.66). Equations (3.18)–(3.27) then lead to the source transfer functions:

$$\tilde{T}^{cs}_\infty = \frac{3}{4A}\left[(w^2-1)(3w^2-1)\log\left(\frac{w+1}{w-1}\right) - 6w\right]; \tag{3.29}$$

$$\tilde{T}^{cs}_0 = \frac{2w}{5A(w^2-1)}; \tag{3.30}$$

$$\tilde{T}^{cc}_{1\infty} = \frac{3}{2}(3w^2-2) + \frac{9}{4}w(w^2-1)\log\left(\frac{w-1}{w+1}\right); \tag{3.31}$$

$$\tilde{T}^{cc}_{10} = \frac{3}{5(w^2-1)}; \tag{3.32}$$

$$\tilde{T}^{cc}_{2\infty} = \tilde{T}^{cs}_\infty; \tag{3.33}$$

$$\tilde{T}^{cc}_{20} = \tilde{T}^{cs}_0 - \frac{4}{3}\tilde{T}^{cr}_{20} = \frac{2}{5A}\left[\frac{w}{w^2-1} - \log\left(\frac{w+1}{w-1}\right)\right]; \tag{3.34}$$

$$\tilde{T}^{cr}_{1\infty} = 0; \tag{3.35}$$

$$\tilde{T}^{cr}_{10} = \frac{3}{5(w^2-1)^2}; \tag{3.36}$$

$$\tilde{T}^{cr}_{2\infty} = 0; \tag{3.37}$$

$$\tilde{T}^{cr}_{20} = \frac{3}{10A}\left[\frac{2w}{w^2-1} - \log\left(\frac{w+1}{w-1}\right)\right] : \tag{3.38}$$

We plot these source transfer functions in Figures 3, 4, and 5. They are now only functions of the initial time, but not of the final time. In the context of topological defects, the defect source was formed at $\eta_i \ll \eta_{eq}$. Therefore it would be also interesting to investigate the asymptotic behaviors of the source transfer functions with very early initial times. For $\eta_i \ll \eta_{eq}$, equations (3.29)–(3.38) become:

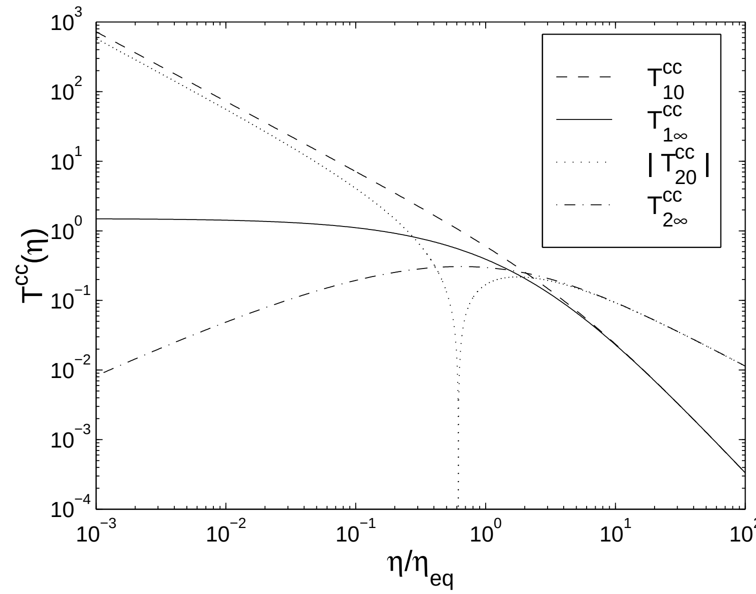

FIG. 4. The source transfer functions $\tilde{T}^{cc}_{10}$ (dashed), $\tilde{T}^{cc}_{11}$ (solid), $\tilde{T}^{cc}_{20}$ (dotted), and $\tilde{T}^{cc}_{21}$ (dot-dashed). We have taken the absolute value of $\tilde{T}^{cc}_{20}$, because it becomes negative when $\eta < 0.6\,\eta_{eq}$.

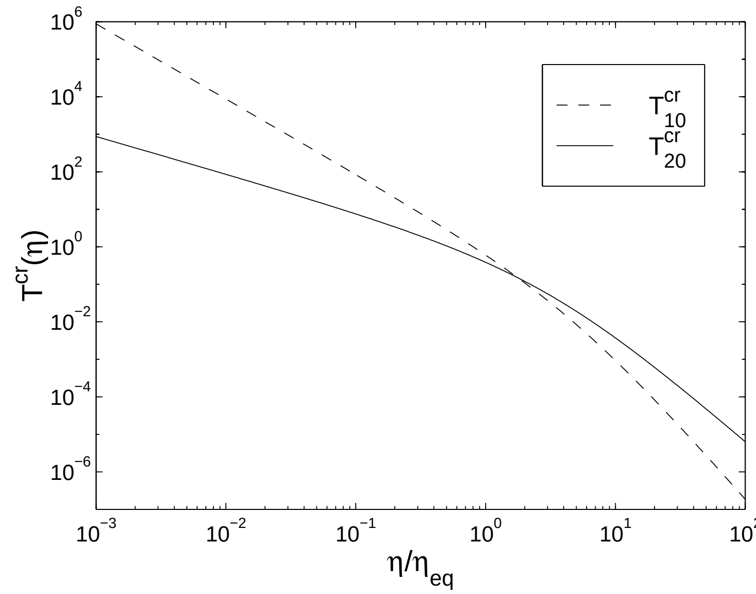

FIG. 5. The source transfer functions $\tilde{T}^{cr}_{10}$ (dashed) and $\tilde{T}^{cr}_{20}$ (solid). We note that $\tilde{T}^{cr}_{11} = \tilde{T}^{cr}_{21} = 0$.

$$\tilde{T}^{cc}_{11\,(i)} = \frac{3}{2}\,; \quad \tilde{T}^{cs}_{1\,(i)} = \tilde{T}^{cc}_{21\,(i)} = \frac{3\,\tau_i}{2\,\tau_{eq}} \log \frac{4\,\tau_{eq}}{A\,\tau_i}\,; \quad \tilde{T}^{cr}_{11\,(i)} = \tilde{T}^{cr}_{21\,(i)} = 0\,; \tag{3.39}$$

$$\frac{3A}{2}\tilde{T}^{cs}_{0\,(i)} = \tilde{T}^{cc}_{10\,(i)} = \frac{3A}{2}\tilde{T}^{cc}_{20\,(i)} = A\frac{\tau_i}{\tau_{eq}}\tilde{T}^{cr}_{10\,(i)} = A\,\tilde{T}^{cr}_{20\,(i)} = \frac{3\,\tau_{eq}}{5A\,\tau_i}\,; \tag{3.40}$$

where the subscript (i) denotes the condition $\tau_i \ll \tau_{eq}$. These asymptotic behaviors can be clearly seen in Figures 3, 4 and 5. We note that on sub-horizon scales, $\tilde{T}^{cs}_1$ has a maximum at $\tau \approx \tau_{eq}$ as seen in Figure 3. Adding the fact that cosmic defects seed matter perturbations only on sub-horizon modes due to the compensation mechanism, it follows that the defect-induced matter perturbations are seeded mainly during the radiation-matter transition era. This is a generically different mechanism from inflationary models, in which matter perturbations are seeded during inflation in the deep radiation era when all the modes are well outside the horizon. Nevertheless, the defect and inflationary models both provide scale-invariant perturbations at horizon crossing, and these perturbations evolve similarly after horizon crossing.

C. Degeneracy of the Green functions

In principle we need ten Green functions (five for $\delta_c = \delta^I_c + \delta^S_c$ and five for $\delta_r = \delta^I_r + \delta^S_r$) in order to solve equations (3.1) and (3.2) by using the formalism (3.8) and (3.9). However, in addition to the dependence (3.14) by which we can reduce the effective number of the Green functions by two, there is another constraint we can invoke — the zero entropy fluctuation on super-horizon scales in the initial conditions, i.e. $s = \dot{s} = 0$ at τ_i for modes $k \ll 1/\tau_i$ (see eqs. [2.18] and [2.49]). Since the formation time τ_i of the active source is normally so early that the condition $k \ll 1/\tau_i$ (and thus $s = \dot{s} = 0$) is generally satisfied on the scales of our cosmological interest, we can rewrite equation (3.8) as

$$\tilde{\delta}^I_N(k;\tau) = \tilde{G}^N_3(k;\tau;\tau_i)\tilde{\delta}_c(k;\tau_i) + \tilde{G}^N_4(k;\tau;\tau_i)\dot{\tilde{\delta}}_c(k;\tau_i)\,; \tag{3.41}$$

where

$$\tilde{G}^N_i \equiv \tilde{G}^N_{i\,2}{}^c + \frac{4}{3}\tilde{G}^N_{i\,2}{}^r\,; \quad i = 3;4\,: \tag{3.42}$$

From equations (3.20), (3.21), (3.24) and (3.25), we can get

$$\tilde{G}^c_{31} = \tilde{G}^{cc}_{11}\,; \quad \tilde{G}^c_{30} = \left[5(w^2-1)^2(y^2-1)^2\right]^{-1}\left(y^6 + 3y^6w^2 - 5y^4 - 15w^2y^4 + 15y^2\right.$$
$$\left. + 45w^2y^2 + 2w^7y - 10w^3y - 6yw^5 - 50yw + 5 + 15w^2\right)\,: \tag{3.43}$$

Using equation (3.14), we can also obtain $\tilde{G}^c_4 = \tilde{G}^{cs}$, so that

$$\tilde{G}^c_{41} = \tilde{G}^{cs}_1\,; \quad \tilde{G}^c_{40} = \tilde{G}^{cs}_0\,: \tag{3.44}$$

These results yield the source transfer functions:

$$\tilde{T}^c_{31} = \tilde{T}^{cc}_{11}\,; \quad \tilde{T}^c_{30} = \frac{3w^2+1}{5(w^2-1)^2}\,; \quad \tilde{T}^c_{41} = \tilde{T}^{cs}_1\,; \quad \tilde{T}^c_{40} = \tilde{T}^{cs}_0\,: \tag{3.45}$$

If the initial time is deep in the radiation era, i.e. $\tau_i \ll \tau_{eq}$, we further have

$$\tilde{T}^c_{30\,(i)} = \frac{4\,\tau^2_{eq}}{5A^2\,\tau^2_i} \propto \tau_i^{-2}\,; \qquad \tilde{T}^c_{31\,(i)} = \tilde{T}^{cc}_{11\,(i)} = \tfrac{3}{2} \propto \tau_i^0\,; \tag{3.46}$$

$$\tilde{T}^c_{40\,(i)} = \tilde{T}^{cs}_{0\,(i)} = \frac{2\,\tau_{eq}}{5A^2\,\tau_i} \propto \tau_i^{-1}\,; \quad \tilde{T}^c_{41\,(i)} = \tilde{T}^{cs}_{1\,(i)} = \tfrac{3\,\tau_i}{2\,\tau_{eq}} \log\tfrac{4\,\tau_{eq}}{A\,\tau_i} \propto \tau_i\,; \tag{3.47}$$

where the last proportionality is only an approximation. Figure 6 shows the solutions of $\tilde{T}^c_{30}$ and $\tilde{T}^c_{31}$ ($= \tilde{T}^{cc}_{11}$), while $\tilde{T}^c_{40} \equiv \tilde{T}^{cs}_0$ and $\tilde{T}^c_{41} \equiv \tilde{T}^{cs}_1$ are already shown in Figure 3. We note the the asymptotic behaviors indicated in equations (3.46) and (3.47) can be clearly seen in Figures 3 and 6. Therefore, the original ten Green functions for solving $\tilde{\delta}_c$ and $\tilde{\delta}_r$ have now been reduced to four functions: two for $\tilde{\delta}_c$ ($\tilde{G}^c_4 \equiv \tilde{G}^{cs}$ and $\tilde{G}^c_3$), and two for $\tilde{\delta}_r$ ($\tilde{G}^r_4 \equiv \tilde{G}^{rs}$ and $\tilde{G}^r_3$). We shall concentrate only on the solutions of $\tilde{\delta}_c$, while leaving those of $\tilde{\delta}_r$ elsewhere [25]. To calculate $\tilde{\delta}^S_c$ we need $\tilde{G}^{cs}$ using equation (3.9); to calculate $\tilde{\delta}^I_c$ we need $\tilde{G}^c_4 = \tilde{G}^{cs}$ and $\tilde{G}^c_3$ using equation (3.41). In solving $\tilde{\delta}^I_c$, we note that $\tilde{G}^c_3$ transfers the initial perturbations of both matter and radiation $[\tilde{\delta}_c(\tau_i) + \tilde{\delta}_r(\tau_i)]$ to today, while $\tilde{G}^{cs}$ transfers the initial perturbations of their time derivatives $[\dot{\tilde{\delta}}_c(\tau_i) + \dot{\tilde{\delta}}_r(\tau_i)]$ to the present.

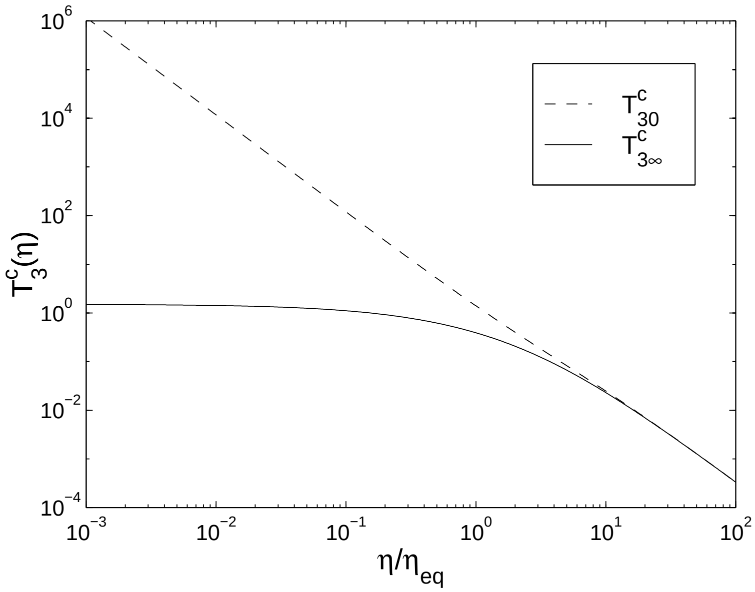

FIG. 6. The source transfer functions $\tilde{T}^c_{30}$ (dashed line) and $\tilde{T}^c_{3\infty}$ ($= \tilde{T}^{cc}_{1\infty}$; solid line).

D. Solutions on intermediate scales

With $\tilde{G}^c_3$ and $\tilde{G}^c_4$ ($= \tilde{G}^{cs}$) as the two basis Green functions, we can now work out the solutions on intermediate scales, using results derived in previous sections. In the matter era, $\tilde{G}^r_i \ll \tilde{G}^c_i$ on all scales so from equation (3.11) we know that $\tilde{G}^c_{i0}(k;\eta_0;\eta_i) = \tilde{G}^c_{i\infty}(k;\eta_0;\eta_i)$ when $\eta_i \gg \eta_{eq}$. This can be clearly seen from Figures 3 and 6. In the radiation era, the perturbations $[\delta_c(\eta_i) + \delta_r(\eta_i)]$ or $[\dot{\delta}_c(\eta_i) + \dot{\delta}_r(\eta_i)]$ that were seeded well before the horizon crossing will evolve in the same way as in the standard CDM model due to the same zero entropy fluctuation initial condition. Therefore the solution interpolating between $\tilde{G}^c_{i0}(k;\eta_0;\eta_i)$ and $\tilde{G}^c_{i\infty}(k;\eta_0;\eta_i)$ for $\eta_i \ll \eta_{eq}$ will be the standard CDM transfer function. Thus we can write down a fit of the solution for the full gamut of k and η_i as

$$\tilde{G}^c_i(k;\eta_0;\eta_i) = \tilde{G}^c_{i\infty}(\eta_0;\eta_i) + \left[\tilde{G}^c_{i0}(\eta_0;\eta_i) - \tilde{G}^c_{i\infty}(\eta_0;\eta_i)\right] T(k) I(k;\eta_i); \quad i = 3,4; \tag{3.48}$$

where

$$T(k) = \left[1 + \frac{(0.0534 + \frac{2.75}{1+3.83k})k^2}{\ln(2e + 0.11k)}\right]^{-1}; \tag{3.49}$$

$$I(k;\eta_i) = \frac{1 + 30\eta_i}{1 + 30\eta_i(1 + \frac{k\eta_i}{2})}; \tag{3.50}$$

and k is in units of η_{eq}^{-1} (see equation (A11)). Here $T(k) \equiv T_c(k;\eta_0;\Omega_{B0} = 0)$ is the standard CDM transfer function without baryons (modified from Ref. [19]; see eq. [2.66] for the definition of $T_c(k;\eta_0)$), and $I(k;\eta_i)$ is a small correction near the horizon crossing to make the analytic solutions (3.48) fit the numerical results. For a given mode which is initially outside the horizon, the background contents of the universe compensate the defect source until horizon crossing. Therefore the detailed behavior of these Green functions near the horizon scale will affect the so-called compensation scale, beyond which no perturbations can grow. This means that the correction function $I(k;\eta_i)$ in equation (3.48) actually plays an important role in getting the compensation scale right, and we shall discuss this further in section IV C. We have verified numerically for both $\tilde{G}^c_3$ and $\tilde{G}^c_4$ that the fit (3.48) is accurate within a 4% error for any k and η_i (note that the initial conditions of $\tilde{G}^c_3$ and $\tilde{G}^c_4$ in the numerical verifications can be obtained from eqs. [3.12], [3.13] and [3.42]). Figure 7 shows the numerical solutions of $\tilde{G}^c_3$ and $\tilde{G}^c_4$ ($= \tilde{G}^{cs}$) within a chosen domain of $(k;\eta_i)$. It confirms the asymptotic behaviors indicated by equations in (3.45) (see also eqs. [3.29], [3.30] and [3.31]), and plotted in Figures 3 and 6. The asymptotic behaviors shown by equations (3.46) and (3.47) can be also marginally observed from Figure 7.

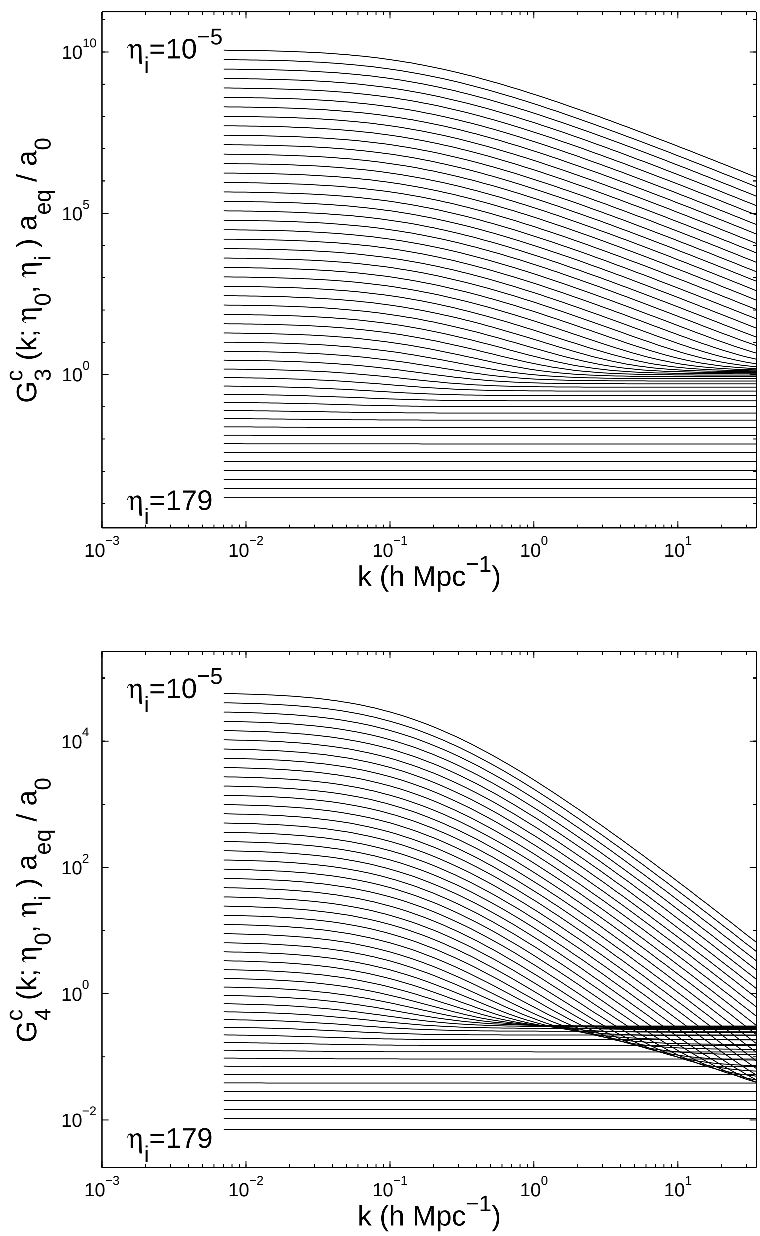

FIG. 7. The numerical solutions of $\mathcal{G}_3^c(k;\eta_0;\eta_i)$ (upper panel) and $\mathcal{G}_4^c(k;\eta_0;\eta_i)$ ($= \mathcal{G}^{cs}(k;\eta_0;\eta_i)$; lower panel). They both have been normalized to the scale factor today, a_0/a_{eq}. Each line has a different initial time η_i, whose smallest and largest values are labeled in both plots. Successive lines have even logarithmic time intervals, and η_i is in units of η_{eq}.

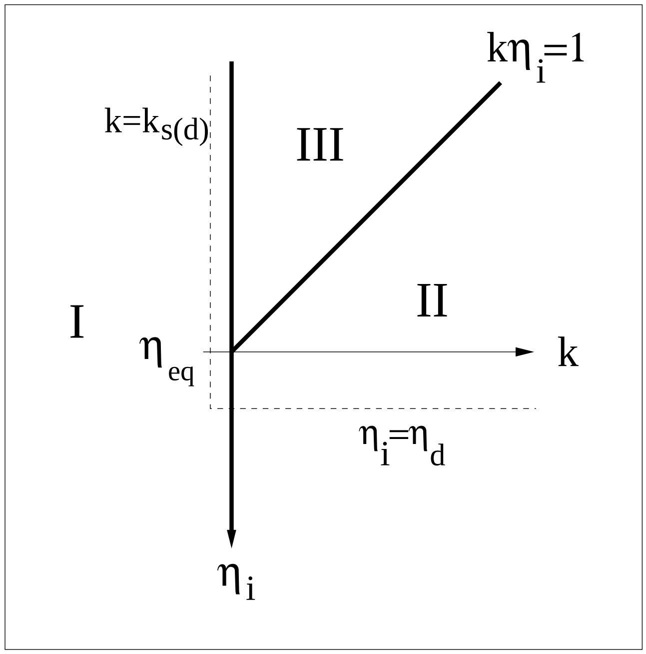

FIG. 8. Three domains on the $(k;\eta_i)$-plane for the solutions of Green functions $\mathcal{G}^c_3$ and $\mathcal{G}^c_4$: Region I ($k < k_{eq} = 1/\eta_{eq}$), Region II ($k > k_{eq}$ and $k > 1/\eta_i$), and Region III ($k_{eq} < k < 1/\eta_i$). These three regions are divided by the thick solid lines. Also shown are the $\eta_i = \eta_d$ (horizontal dashed line), and the $k = k_{s(d)}$ (vertical dashed line).

Schematically, we can divide the $(k;\eta_i)$-plane into three regions for the solutions of $\mathcal{G}^c_i$ ($i = 3;4$). As shown in Figure 8, these three domains are: Region I ($k < k_{eq} = 1/\eta_{eq}$), Region II ($k > k_{eq}$ and $k > 1/\eta_i$), and Region III ($k_{eq} < k < 1/\eta_i$). In Region I, the solution of $\mathcal{G}^c_i$ is $\mathcal{G}^c_{i0}$ because the horizon crossing happens after η_{eq}, after which $\mathcal{G}^c_{i0} = \mathcal{G}^c_{i1}$ as argued before. In Region II, the solution is $\mathcal{G}^c_{i1}$ because all modes in this region are inside the horizon all the time. We notice that $\mathcal{G}^c_{i0}$ merges with $\mathcal{G}^c_{i1}$ at the boundary of Regions I and II, where $\eta_i > \eta_{eq}$. In Region III, the solution along the k direction is in the same form as the standard CDM transfer function. This is because modes with larger k cross the horizon earlier, so that their perturbations are suppressed after the horizon crossing for longer until η_{eq}. In addition, the solution along the η_i direction in Region III is in the same form as $\mathcal{G}^c_{i0}$. This is because modes in this region are initially on super-horizon scales, and a given mode with different initial time η_i will experience the same amount of suppression resulting from the period between the horizon crossing and η_{eq}. Therefore, Regions I, II and III illustrate the intrinsic property of the solution (3.48).

E. The effect of baryons

There is one important issue which we have not discussed — the effect of baryons. Prior to the photon-baryon decoupling at η_d, the CDM and baryons are dynamically independent. In this era, the photon-baryon fluid propagates as acoustic waves with a sound speed given by equation (2.11), preventing baryons from collapsing on small scales. Therefore there exists a sound horizon at the decoupling epoch $d_{s(d)}$ (hereafter simply the sound horizon) which is the distance such waves can travel prior to η_d, and which is the largest scale at which the baryons can affect the evolution of density perturbations. It has been shown that inside the sound horizon $d_{s(d)}$, not only are the CDM perturbations seeded before η_d suppressed due to the presence of baryons (e.g. [24,19,21]), but also the baryons themselves have an exponentially decaying power due to the Silk damping [22] (see also eq. [2.53]), with acoustic oscillations due to the velocity overshoot [26,27]. After the decoupling, baryons evolve in the same way as the CDM does, so the matter perturbations today can be obtained by linearly combining the CDM and baryonic fluctuations at η_d (see section IIF and eq. [2.65]), and then evolving them to today.

It follows that the baryonic effects tend to suppress the matter perturbations seeded before the decoupling epoch ($\eta < \eta_d$, see the horizontal dashed line in Figure 8) and on scales inside the sound horizon (i.e. for $k > k_{s(d)} \equiv 1/d_{s(d)}$, see the vertical dashed line in Figure 8). The perturbations seeded after η_d or on scales $k < k_{s(d)}$ will not be affected by the baryons. With this argument, we can impose a suppression factor on our current solution (3.48) to account for the effect of baryons, i.e. the solution with the inclusion of baryons can be written as

$$\tilde{\mathcal{G}}_i^{c(B)}(k;\tau;\tau_i;h;\Omega_{m0};\Omega_{B0}) = \tilde{\mathcal{G}}_i^{c}(k;\tau;\tau_i)B(k;\tau_i;h;\Omega_{m0};\Omega_{B0}); \tag{3.51}$$

where $B(k;\tau_i;h;\Omega_{m0};\Omega_{B0})$ accounts for the baryonic suppression:

$$B(k;\tau_i;h;\Omega_{m0};\Omega_{B0}) = \begin{cases} \frac{T(k;h;\Omega_{m0};\Omega_{B0})}{T(k;h;1;0)}; & \text{for } \tau_i \ll \tau_d; \\ 1; & \text{for } \tau_i > \tau_d \text{ or } k < k_{s(d)} \approx 1/d_{s(d)}; \end{cases} \tag{3.52}$$

where $T(k;h;\Omega_{m0};\Omega_{B0})$ is the usual standard CDM transfer function with the baryonic dependence. One accurate fit of $T(k;h;\Omega_{m0};\Omega_{B0})$ is provided in Ref. [19]. We note that the ratio $T(k;h;\Omega_{m0};\Omega_{B0})/T(k;h;1;0)$ is unity outside the sound horizon ($k < k_{s(d)} \approx 1/d_{s(d)}$), and is less than unity inside the sound horizon. Referring to Figure 8, equation (3.52) means that the value of $B(k;\tau_i;h;\Omega_{m0};\Omega_{B0})$ is less than unity in the region to the right and above the dashed lines, and is unity otherwise. We also note that in the low-Ω_{m0} models, the sound horizon can be smaller than the radiation-matter equality horizon, i.e., it is possible that $k_{s(d)} \approx 1/d_{s(d)} > k_{eq}$ [19]. In addition, there is a transition era ($\tau_i < \tau_d$) which is not included in equation (3.52). This is because in this era the baryonic effects do not fully operate as in the regime $\tau_i \ll \tau_d$ so that a good fit is not trivial to obtain. We have numerically verified equation (3.52), although an accurate fit to the missing era $\tau_i < \tau_d$ has yet to be found.

F. Solutions in $K \neq 0$ or $\Lambda \neq 0$ models

The solutions we have obtained so far have assumed $K = \Lambda = 0$. For $K \neq 0$ or $\Lambda \neq 0$, the growing behavior of the CDM perturbations departs from that of a flat $\Lambda = 0$ model only at very late times in the matter era (see later for a more detailed argument). This allows us to apply a universal suppression factor on $\tilde{\mathcal{G}}^{c(B)}$ to account for the effects of curvature or Λ:

$$\tilde{\mathcal{G}}_i^{c(B)}(k;\tau_0;\hat{\tau};h;\Omega_{m0};\Omega_{B0};\Omega_{\Lambda 0}) = \Omega_{m0}h^2 g(\Omega_{m0};\Omega_{\Lambda 0})\tilde{\mathcal{G}}_i^{c(B)}(k;\tau_0;\hat{\tau};1;1;\Omega_{B0};0); \tag{3.53}$$

where k is in units of $\Omega_{m0}h^2\,\mathrm{Mpc}^{-1}$, and $g(\Omega_{m0};\Omega_{\Lambda 0})$ is given by [28]

$$g(\Omega_{m0};\Omega_{\Lambda 0}) = \frac{5\Omega_{m0}}{2}\left[\Omega_{m0}^{4/7} - \Omega_{\Lambda 0} + (1+\Omega_{m0}/2)(1+\Omega_{\Lambda 0}/70)\right]^{-1}: \tag{3.54}$$

In equation (3.53), the leading factor $\Omega_{m0}h^2$ results from the fact that the ratio of scale factors a_0/a_{eq} is proportional to $\Omega_{m0}h^2$ and that the Green function $\tilde{\mathcal{G}}_i^{c(B)} = \tilde{\mathcal{F}}_i^{c(B)}a_0/a_{eq}$ is proportional to this ratio. The factor $g(\Omega_{m0};\Omega_{\Lambda 0})$ accounts for the suppression of the linear growth of density perturbations in a $K \neq 0$ or Λ-universe relative to an $\Omega_{m0} = 1$ and $\Omega_{\Lambda 0} = 0$ universe [28] (also verified in Ref. [29]). The reason for k to have the unit $\Omega_{m0}h^2\,\mathrm{Mpc}^{-1}$ in equation (3.53) is that the horizon size at radiation-matter equality τ_{eq} is proportional to $(\Omega_{m0}h^2)^{-1}$ (see eq. [A11] in Appendix A).

For $K \neq 0$ or $\Lambda \neq 0$, the extrapolation scheme (3.53) will be inaccurate when $\hat{\tau}$ is close to τ_0, i.e., when the background dynamics at $\hat{\tau}$ significantly departs from that of a flat $\Lambda = 0$ model. Nevertheless, this extrapolation scheme is still appropriate for most models with active source for two reasons. First, in the context of cosmic defects, the power of matter perturbations on the scales of our interest ($k \approx 0.01$–$1h\,\mathrm{Mpc}^{-1}$) is mainly seeded around τ_{eq} (see Figure 10 and the discussion after eq. [3.40]). At this time, the curvature or Λ effects are negligible. Second, at late times when the curvature or Λ effects become important, these scales of our interest are already well inside the horizon so that any curvature terms in the perturbation equations can be neglected. Therefore, the only required change in the perturbation equations to account for the effects of curvature or Λ is simply to incorporate the correct background dynamics, and this involves only modifications in $a(\tau)$, $\rho_c(\tau)$ and $\rho_r(\tau)$, whose solutions are given in Appendix A. As can be seen in Figure 10, the presence of curvature or a cosmological constant affects the background dynamics only at late times. More precisely, we verify that for $(\Omega_{m0};\Omega_{\Lambda 0}) = (0.2;0);(0.2;0.8);(1;0)$ and $(2.0;0)$, the largest observable scale for matter perturbations $k \approx 0.01h\,\mathrm{Mpc}^{-1}$ corresponds to the horizon sizes at $\tau \approx 5;5;27;54\,\tau_{eq}$ respectively, whereas in these models the curvature or cosmological-constant domination occurs only at a much later epoch when $\tau > \tau_0$. At these moments ($\tau \approx 5;5;27;54\,\tau_{eq}$), the scale factor in the $K \neq 0$ or $\Lambda \neq 0$ models departs from that in the flat $\Lambda = 0$ model only by less than one percent. Indeed, we have numerically verified that the extrapolation scheme (3.53) is accurate within a 5% error for $\tau_i \lesssim 60\,\tau_{eq}$ and $\Omega_\Lambda \lesssim 0.85$ in Λ-models, for $\tau_i \lesssim 20\,\tau_{eq}$ and $\Omega_{m0} \gtrsim 0.2$ in open $\Lambda = 0$ models, and for $\tau_i \lesssim 200\,\tau_{eq}$ and $\Omega_{m0} \lesssim 2$ in closed $\Lambda = 0$ models. These ranges of cosmological parameters have apparently covered the values of our interest.

IV. IMPORTANT PROPERTIES

With the Green-function solutions we have found, we can now analytically investigate some important aspects about the growth of cosmological matter perturbations.

A. The standard CDM model

First we investigate the relationship between our Green functions and the standard CDM transfer function, and thereby to justify the use of the standard CDM transfer function in the analytic solution (3.48). In the standard CDM model, there are no subsequent perturbations, so we have $\tilde{\delta}_N = \tilde{\delta}^I_N + \tilde{\delta}^S_N = \tilde{\delta}^I_N$. As discussed in equations (2.36) and (2.37), we also know that the CDM perturbations have a growing mode $\tilde{\delta}_c(k;\tau) \propto \tau^2$ on super-horizon scales ($k\tau \ll 1$) for $\tau \ll \tau_{eq}$ or $\tau \gg \tau_{eq}$. For the super-horizon modes in the radiation era and all modes in the matter era, this allows us to write

$$\tilde{\delta}_c(k;\tau) = A_j(k)\,\tau^2; \quad j = R, M; \tag{4.1}$$

where A_j is the coefficient of the growing mode in the radiation era ($j = R$: $\tau \ll \tau_{eq}$ and $k\tau \ll 1$) or in the matter era ($j = M$: $\tau \gg \tau_{eq}$). Thus using our Green-function solutions (3.41) and (3.48) with the initial conditions $s = \underline{s} = 0$ and $\dot{\tilde{\delta}}_N(k;\tau_i) = 2\tilde{\delta}_N(k;\tau_i)/\tau_i$ as required by the adiabatic inflationary model, we can derive the standard CDM transfer function as

$$\begin{aligned}\frac{A_M}{A_R} &= \frac{\tilde{\delta}^I_c(k;\tau)\,\tau_i^2}{\tilde{\delta}_c(k;\tau_i)\,\tau^2} = \frac{A^2\tau_i^2 a_{eq}}{4\tau_{eq}^2 a}\left(\tilde{G}^c_3 + \frac{2}{\tau_i}\tilde{G}^c_4\right)\\ &= \frac{1}{4\tau_{eq}^2}\left[A^2\tau_i^2\tilde{F}^c_{30(i)} + 2A^2\tau_i\tilde{F}^c_{40(i)}\right]T(k) = \frac{2}{5}T(k);\end{aligned} \tag{4.2}$$

where we have used $\tau_i \ll \tau_{eq}$ and equations (A13), (3.28), (3.46) and (3.47), and the last expression was obtained based on the formalism (3.48). First, we note that the two terms involving $\tilde{F}^c_{30(i)}$ and $\tilde{F}^c_{40(i)}$ are equal, meaning that the two sets of initial perturbations $[\tilde{\delta}_c(\tau_i) + \tilde{\delta}_r(\tau_i)]$ and $[\dot{\tilde{\delta}}_c(\tau_i) + \dot{\tilde{\delta}}_r(\tau_i)]$ contribute equally to the present matter perturbations. Second, the $T(k)$ here is nothing but the standard CDM transfer function which we have defined earlier. Third, the coefficient $2/5$ in the final result of equation (4.2) is well known (e.g. [17,24]), and here we obtained it using our Green-function solutions. This coefficient can be also obtained by first knowing from equation (2.45) that Φ_{00} is a constant on super-horizon scales ($k \ll 1/\tau$), and then using its definition (2.38) and equation (4.1) to compare its expressions for $j = R, M$. One will find $\Phi_{00} = A_R = \pi G = 5A_M = 2\pi G$, which implies $A_M/A_R = 2/5$ for $k \ll 1/\tau$. Thus the above derivation and result not only illustrate the relation between our Green functions and the the standard CDM transfer function $T(k)$, but also justify the use of $T(k)$ in our formalism (3.48).

B. Independence of the initial conditions

One important problem for structure formation with causal seeds is to investigate how the source energy was compensated into the radiation and matter background when the seeds were formed at τ_i. From the result (2.48) we know that the power spectrum of the pseudo energy $\tilde{\Theta}_{00}$ should decay as k^4 on super-horizon modes. As argued in equation (2.49), we can thus take $\tilde{\Theta}_{00} = 0$ as part of the initial conditions provided that the scales of interest are well outside the horizon initially. For similar reasons we can take $\tilde{s} = \dot{\tilde{s}} = 0$, where $s = 3\delta_r/4 - \delta_c$. In addition, from equation (2.38) without baryons, we have

$$\Theta_{00} = \Theta_{00} + \frac{3}{8\pi G}\left(\frac{\dot{a}}{a}\right)^2 \sum_{N=c,r} \rho_N\delta_N + \frac{1}{4\pi G}\frac{\dot{a}}{a}\dot{\delta}_c. \tag{4.3}$$

Since $\Theta_{00} = 0$ is required at τ_i, it follows that for a given $\Theta_{00}(x;\tau_i)$, one can have different ways of compensating it into between δ_N and $\dot{\delta}_N$. It is thus vital to check the dependence of the resulting $\delta^I_c(\tau)$ on the way we compensate $\Theta_{00}(x;\tau_i)$ into the background initially. Consider the following two extreme cases, both satisfying $\tilde{\Theta}_{00} = \tilde{s} = \dot{\tilde{s}} = 0$ on super-horizon scales at τ_i:

1. $\tilde\delta_c = 3\tilde\delta_r/4 = 0$, $\dot{\tilde\delta}_c = 3\dot{\tilde\delta}_r/4 = [-4\pi G(a/\dot a)\tilde\Theta_{00}]_i$: Using equation (3.41), the normalized resulting initial perturbations can be calculated as

$$\Delta_1(\tau;\tau_i) = \frac{\tilde\delta_c^I(k;\tau)}{[-4\pi G(a/\dot a)\tilde\Theta_{00}]_i} = \tilde G_4^c = \tilde G^{cs}: \tag{4.4}$$

2. $\tilde\delta_c = 3\tilde\delta_r/4 = [-8\pi G(a/\dot a)^2\tilde\Theta_{00}/(4-\Omega_c)]_i$, $\dot{\tilde\delta}_c = 3\dot{\tilde\delta}_r/4 = 0$: Similarly we have

$$\Delta_2(\tau;\tau_i) = \frac{\tilde\delta_c^I(k;\tau)}{[-4\pi G(a/\dot a)\tilde\Theta_{00}]_i} = \tilde G_3^c\frac{2w(w^2-1)}{A(3w^2+1)}: \tag{4.5}$$

To see the difference in $\tilde\delta_c^I(k;\tau_0)$ today resulting from these two cases, one can calculate

$$D_{12}(\tau_0;\tau_i) = \frac{\Delta_2}{\Delta_1} - 1 = \frac{2w(w^2-1)}{A(3w^2+1)}\frac{\tilde F^c_{30}}{\tilde F^{cs}_0} = 0; \tag{4.6}$$

where we have used equations (3.30), (3.45) and (3.48). This implies that no matter how the source $\Theta_{00}(x;\tau_i)$ is compensated into the background when it was formed (i.e. with any portions between ρ_N and $\rho_{\bar N}$ initially), it results in the same $\tilde\delta_c^I(k;\tau_0)$ today on scales which were outside the horizon at τ_i. We note that this independence of the initial conditions was first numerically observed in Ref. [17], and here we have provided an analytic proof.

C. Compensation and total matter perturbations

With a complete set of Green functions for both initial and subsequent perturbations, we can now investigate the resulting total CDM perturbations and therefore the compensation mechanism in models with active source. Having seen the independence of the resulting $\tilde\delta_c^I(k;\tau_0)$ on the way the source energy is initially compensated into various background components, we can invoke equation (4.4) for $\tilde\delta_c^I$, and equation (3.9) for $\tilde\delta_c^S$ to obtain $\tilde\delta_c(k;\tau_0) = \tilde\delta_c^I(k;\tau_0) + \tilde\delta_c^S(k;\tau_0)$. For a given mode at which $k\tau_i \ll 1$ initially, we have:

$$\begin{aligned}
\tilde\delta_c(k;\tau_0) &= \tilde\delta_c^I(k;\tau_0) + \tilde\delta_c^S(k;\tau_0) \\
&= 4\pi G\left\{-\frac{a(\tau_i)}{\dot a(\tau_i)}\tilde G^{cs}(k;\tau_0;\tau_i)\tilde\Theta_{00}(k;\tau_i) + \int_{\tau_i}^{\tau_0}\tilde G^{cs}(k;\tau_0;\hat\tau)\tilde\Theta_+(k;\hat\tau)d\hat\tau\right\} &(4.7)\\
&= \frac{8\pi G a_0}{5A^2 a_{eq}}\left\{-T(k)\tilde\Theta_{00}(k;\tau_i) + \int_{\tau_i}^{\tau_0}T'(k;\hat\tau)\frac{\dot a(\hat\tau)}{a(\hat\tau)}\tilde\Theta_+(k;\hat\tau)d\hat\tau\right\} &(4.8)\\
&= \frac{8\pi G a_0}{5A^2 a_{eq}}\Big\{-T(k)\tilde\Theta_{00}(k;\tau_0) + \\
&\quad \int_{\tau_i}^{\tau_0}\left[T'(k;\hat\tau)\frac{\dot a(\hat\tau)}{a(\hat\tau)}\tilde\Theta_+(k;\hat\tau) + T(k)\dot{\tilde\Theta}_{00}(k;\hat\tau)\right]d\hat\tau\Big\}; &(4.9)
\end{aligned}$$

where

$$T'(k;\hat\tau) = \frac{\tilde G_4^c(k;\tau_0;\hat\tau)}{\tilde G_{40}^c(k;\tau_0;\hat\tau)}; \tag{4.10}$$

and $\tilde G_4^c(k;\tau_0;\hat\tau)$ is given by (3.48). The function $T'(k;\hat\tau)$ is plotted in Figure 9. Here we notice that the quantities inside the outermost brackets in equations (4.8) and (4.9) are equivalent to nothing but the coefficient of the growing mode in CDM perturbations. Using equation (4.8), one can obtain the resulting perturbations $\tilde\delta_c(k;\tau_0)$ by knowing the initial $\tilde\Theta_{00}(k;\tau_i)$ and integrating the evolution history of $\tilde\Theta_+(k;\hat\tau)$. Hence this expression is convenient for numerical purposes. In addition, we see that the first term in equation (4.8) comes simply from the initial source energy, serving with an opposite sign to account for energy conservation. This is the so-called compensation. On the other hand, the

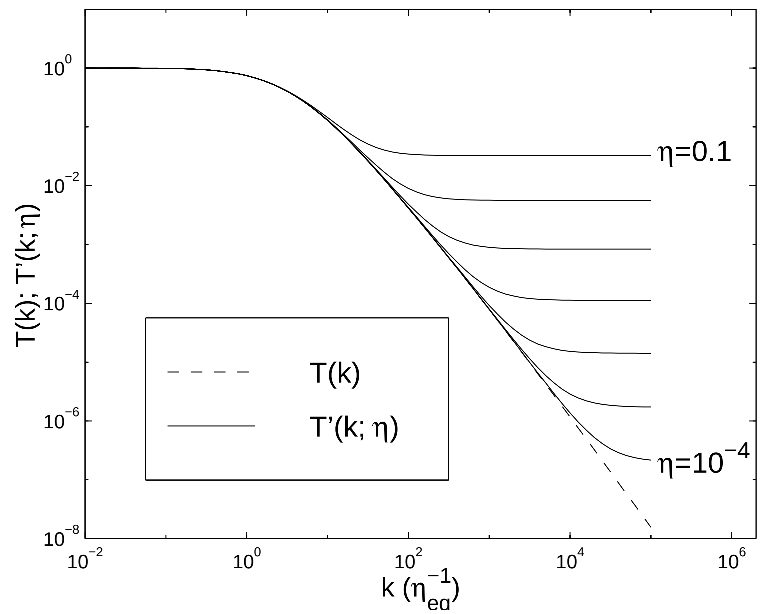

FIG. 9. The function $T'(k;\eta)$ (solid lines) and the standard CDM transfer function $T(k)$ (the dashed line). Each solid line has different η, whose highest and lowest values are labeled in units of η_{eq}. Successive lines have even logarithmic time intervals.

second term results from the subsequent evolution of $\tilde{\Theta}_+(k;\hat\eta)$, which actively creates the CDM density perturbations on sub-horizon scales (see later). This term also provides a way for defects to create non-Gaussianity.

Alternatively, equation (4.9) provides a both physically and mathematically transparent way of interpreting how the perturbations are seeded by the source. First consider the integral term for a given mode k. When the mode is well outside the horizon, i.e. $\hat\eta \ll 1/k$, $T'(k;\eta)$ equals $T(k)$ by definition. Hence the two terms inside the inner brackets reduce to $\tilde{\Theta}_{0i,i}(k;\hat\eta)T(k)$ due to source stress-energy conservation (2.21). Since the power spectrum of $\tilde{\Theta}_{0i,i}(k;\hat\eta)$ falls off as k^4 outside the horizon (see eq. [2.47]), we expect the quantity inside the brackets to be negligible until the given mode approaches horizon crossing. Near horizon crossing, $\tilde{\Theta}_{0i,i}(k;\hat\eta)$ is no longer small, and $T'(k;\eta)$ starts departing from $T(k)$ (i.e. $T'(k;\eta) \sim$ constant $> T(k) \propto k^{-2}$, see Figure 9), so the two terms inside the inner brackets begin to contribute to the integral. This also explains why the correction function $I(k;\eta_i)$ in equation (3.48) is important in affecting the compensation scale. After horizon crossing, the significance of the two terms inside the inner brackets then depends on the subhorizon behaviours of their power spectra.

As for the first term in equation (4.9), we see that for a superhorizon mode today, the integral in (4.9) is negligible as argued above so that only the first term contributes. It serves to give the opposite sign to the source energy so as to account for energy conservation on superhorizon scales today, and thus for the compensation at the present epoch η_0. On the other hand, if a given mode is well inside the horizon today, then the first term will be negligible provided that the source energy $\tilde{\Theta}_{00}(k;\eta_0)$ has a power-law fall-off inside the horizon, as it does for cosmic strings. Therefore in calculating CDM perturbations on scales of our interest, which are well inside the horizon today, the first term in equation (4.9) is negligible, so that it will not affect our compensation argument observed from the integral.

This argument can be further strengthened by deriving the pseudo-energy today. From the definition of τ_{00} (4.3) and the final result of equation (4.9), one obtains

$$\tilde{\tau}_{00}(k;\eta_0) = (1 - T(k))\tilde{\Theta}_{00}(k;\eta_0) + \int_{\eta_i}^{\eta_0} \left[T'(k;\hat\eta)\frac{\dot{a}(\hat\eta)}{a(\hat\eta)}\tilde{\Theta}_+(k;\hat\eta) + T(k)\dot{\tilde{\Theta}}_{00}(k;\hat\eta) \right] d\hat\eta . \quad (4.11)$$

From this result, one can clearly see that for super-horizon modes, $T(k)$ is unity by definition so that only the integral survives. We have also seen from an earlier argument that on super-horizon scales, the quantity inside the square brackets is nothing but the $\tilde{\Theta}_{0i,i}(k;\hat\eta)$, which has a k^4 fall-off power spectrum (see eq. [2.47]). It follows immediately from equation (4.11) that the pseudo-energy today, $\tau_{00}(\eta_0)$, has a k^4-decay power spectrum outside the horizon. This result confirms the super-horizon behavior of τ_{00} presented in equation (2.48). On the other hand, although $(1 - T(k))$

is approximately unity for sub-horizon modes, the usual sub-horizon power-law decay in $\Theta_{00}(k;\tau_0)$ (as in the case of cosmic strings) will still make the first term in equation (4.11) negligible inside the horizon.

Thus we can see explicitly in a neat mathematical form how compensation acts on a given length-scale. From this analysis we can also see that the compensation scale is determined not only by the functions $T^0(k;\tau)$ and $T(k)$, but also by the properties of the source near the horizon scale. Once the detailed behavior of the source near the horizon scale is known, we can accurately locate the compensation scale using equation (4.9) or (4.11). We note that this result is different from the claim in Ref. [30], where multi-fluid compensation back-reaction effects were studied to show that the compensation scale arises naturally and uniquely from an algebraic identity in the perturbation analysis. Ref. [31] also investigated the compensation scale, and found constraints on the generation of super-causal-horizon energy perturbations from a smooth initial state, under a simple physical scheme. The compensation wavenumber was found to be constrained with $k_c > 2\tau^{-1}$ due to causality, depending on the behavior of the causal events. This result is not inconsistent with our finding above, where we further provide a quantitative way to locate the compensation scale for any given specific model.

V. SUMMARY AND CONCLUSION

In this paper we present a formalism which can be used to study the evolution of cosmological perturbations in the presence of causal seeds. In this formalism we invoked the fluid approximation in the synchronous gauge to model the contents of the universe, and assumed photon-baryon tight coupling until the last-scattering epoch to account for the baryonic effects. The approximation of instantaneous decoupling of photons and baryons was then employed at the last-scattering epoch. In particular, we demonstrated the accuracy of our formalism in the context of the standard CDM model, by comparing our results of density perturbations with those calculated from CMBFAST.

We then derived the analytic solutions of matter density perturbations in a flat $\Lambda = 0$ cosmology. The errors in Ref. [16] were corrected to yield a complete set of Green-function solutions for the super-horizon and sub-horizon modes (eqs. [3.3], [3.8], [3.9], [3.18]–[3.40]). The degeneracy among these Green functions was then found by comparing their initial conditions and employing the zero-entropy initial condition (eqs. [3.14], [3.41]). This effectively reduces the number of the Green functions needed in the perturbation solutions (eqs. [3.3], [3.9], [3.41]–[3.47]). With this great simplification, the solutions on intermediate scales were then easily found by the use of the standard CDM transfer function (eq. [3.48]). This complete set of solutions were numerically verified to high accuracy. The baryonic effects were also considered (eq. [3.51]). We then extrapolated these Green-function solutions to $K \neq 0$ or $\Lambda \neq 0$ models (eq. [3.53]), with numerical justifications to high accuracy.

Using these Green-function solutions, we investigated several important aspects of structure formation with causal source. We first demonstrated the relation between our Green functions and the standard CDM transfer function (eq. [4.2]). Second we proved that the resulting matter perturbations today is independent of the way the source was initially compensated into the background contents of the universe (eq. [4.6]). With our Green-function solutions and the use of the pseudo-stress-energy tensor, we finally addressed the compensation mechanism in a mathematically and physically explicit way (eqs. [4.8], [4.9], [4.11]). In particular, the compensation scale was shown to be dependent not only on the dynamics of the universe, but also on the properties of the source near the horizon scale. Once given the detailed behavior of the source near the horizon scale, the compensation scale can be accurately located using our Green functions (eq. [4.11]).

Although in the literature, there have been detailed treatments of theories with causal seeds, the formalism and its analytic solutions presented here will provide not only a physically transparent way for understanding the evolution of matter perturbations, but also a computationally economical scheme which is particularly pertinent when one needs to investigate the phase information of the resulting cosmological perturbations. Following the same line of development, we have been also working on the analytic solutions for radiation perturbations [25], which will be useful in computing the full-sky CMB anisotropies seeded by topological defects. Finally, we note that although we have been concentrating on investigating the perturbations with causal source, our Green-function solutions are completely general and therefore can be also applied to the study of models with acausal source.

Acknowledgments— We thank Andrew Liddle, Paul Shellard, Radek Stompor, and Neil Turok for useful conversations. We acknowledge support from NSF KDI Grant (9872979) and NASA LTSA Grant (NAG5-6552).

[1] A.H. Guth, Phys. Rev. D 23, 347 (1981)
[2] For a review see A. Vilenkin & E. P. S. Shellard, 'Cosmic strings and other topological defects', Cambridge University Press, Cambridge (1994)
[3] P.P. Avelino, E.P.S. Shellard, J.H.P. Wu & B. Allen, Phys. Rev. Lett. 81, 2008 (1998)
[4] P.P. Avelino, E.P.S. Shellard, J.H.P. Wu & B. Allen, Astrophys. J. 507, L101 (1998)
[5] J.H.P. Wu, P.P. Avelino, E.P.S. Shellard & B. Allen, 'Cosmic Strings, Loops, and Linear Growth of Matter perturbations' (see astro-ph/9812156)
[6] U.L. Pen, U. Seljak & N. Turok, Phys. Rev. Lett. 79, 1615 (1997)
[7] A. Albrecht, R.A. Battye & J. Robinson, Phys. Rev. Lett. 79, 4736 (1997)
[8] R.A. Battye, A. Albrecht & J. Robinson, Phys. Rev. Lett. 80, 4847 (1998)
[9] C. Contaldi, M. Hindmarsh & J. Magueijo, Phys. Rev. Lett. 82, 679 (1999)
[10] P.P. Avelino, R.R. Caldwell & C.J.A.P. Martins, Phys. Rev. D 56, 4568 (1997)
[11] B. Allen, R.R. Caldwell, S. Dodelson, L. Knox, E.P.S. Shellard & A. Stebbins, Phys. Rev. Lett. 79, 2624 (1997)
[12] R. Durrer, M. Kunz & A. Melchiorri, Phys. Rev. D 59, 123005 (1999)
[13] U. Seljak & M. Zaldarriaga, Astrophys. J. 469, 437 (1996)
[14] W. Hu, U. Seljak, M. White & M. Zaldarriaga, Phys. Rev. D 57, 3290 (1998)
[15] W. Hu & M. White, Phys. Rev. D 56, 596 (1997)
[16] S. Veeraraghavan & A. Stebbins, Astrophys. J. 365, 37 (1990)
[17] U. Pen, D. Spergel & N. Turok, Phys. Rev. D 49, 692 (1994)
[18] We thank N. Turok for providing the idea of spliting the photon and baryon components here.
[19] D.J. Eisenstein & W. Hu, Astrophys. J. 496, 605 (1998)
[20] W. Hu & N. Sugiyama, Astrophys. J. 444, 489 (1995)
[21] W. Hu & N. Sugiyama, Astrophys. J. 471, 542 (1996)
[22] J. Silk, Astrophys. J. 151, 459 (1968)
[23] R.A. Battye, Phys. Rev. D 55, 7361 (1997)
[24] J.R. Bond & G. Efstathiou, Astrophys. J. 285, L45 (1984)
[25] J.H.P. Wu, in preparation.
[26] R. Sunyaev & Ya.B. Zel'dovich, Ap&SS, 7, 3 (1970)
[27] W. Press & E. Vishniac, Astrophys. J. 236, 323 (1980)
[28] S.M. Carroll, W.H. Press & E.L. Turner, Annu. Rev. Astron. Astrophys. 30, 499 (1992)
[29] D.J. Eisenstein, 'An Analytic Expression for the Growth Function in a Flat Universe with a Cosmological Constant' (see astro-ph/9709054)
[30] C. Cheung & J. Magueijo, Phys. Rev. D 56, 1982 (1997)
[31] J. Robinson & B.D. Wandelt, Phys. Rev. D 53, 618 (1996)
[32] A.A. Penzias & R.W. Wilson, Astrophys. J. 142, 419 (1965)
[33] K.C. Jacobs, Nature (London) 215, 1156 (1967)
[34] J.M. Cohen, Nature (London) 216, 249 (1967)
[35] A.D. Chernin, Nature (London) 220, 250 (1968)
[36] C.B.G. McIntosh, Mon. Not. R. Astron. Soc. 140, 461 (1968)
[37] E.W. Kolb & M.S. Turner, 'The Early Universe', Addison-Wesley, Redwood City, California (1990)

APPENDIX A: COSMOLOGICAL BACKGROUND DYNAMICS

With the discovery of the CMBR in 1964 [32], the universe is believed to be mainly composed of not only matter but also radiation. After the discovery, several authors worked out the solutions in some FRW models with both radiation and matter [33–36]. In this appendix, we aim to derive the general solution of FRW models, in the presence of both curvature and a cosmological constant.

We assume that the universe is homogeneous and isotropic, and is filled with two fluids, radiation and dark matter, whose stress-energy tensors are also homogeneous and isotropic on average. We shall ignore the overall contribution of the stress energy from causal seeds like defect fields, because in general they are much smaller than the total energy density of radiation and matter. Thus in a FRW universe with only radiation and matter components that evolve independently and adiabatically, the scale factor $a(\tau)$ is determined by the unperturbed Einstein equation, or equivalently the Friedmann equation:

$$\dot{a}^2 + K a^2 = \frac{8\pi G \rho_{m0} a_0^3}{3}(1+a) + \frac{\Lambda}{3}a^4; \tag{A1}$$

where a dot represents a derivative with respect to the conformal time τ, K is the curvature, ρ_m is the matter energy density, Λ is the cosmological constant, and we have normalized $a_{eq} = 1$. If we define

$$\Omega_m = \frac{8\pi G \rho_m}{3H^2}; \tag{A2}$$

$$\Omega_r = \frac{8\pi G \rho_r}{3H^2} = \frac{8\pi G \rho_m}{3aH^2}; \tag{A3}$$

$$\Omega_\Lambda = \frac{\Lambda}{3H^2}; \tag{A4}$$

$$\Omega_K = -\frac{K}{a^2H^2}; \tag{A5}$$

where $H = \dot{a}/a^2$ is the Hubble parameter, then we have from (A1) that $\Omega_m + \Omega_r + \Omega_\Lambda + \Omega_K = 1$ and

$$\frac{\Omega_{\Lambda 0}}{\Omega_{m0}} = \frac{\Lambda}{8\pi G \rho_{m0}}; \quad \frac{\Omega_{K0}}{\Omega_{m0}} = -\frac{3K}{8\pi G \rho_{m0} a_0^2}. \tag{A6}$$

We also notice that $\Omega_{r0}/\Omega_{m0} = a_0^{-1} \ll 1$. We define

$$A = \frac{2(\sqrt{2}-1)}{\eta_{eq}}; \quad B = \frac{\Omega_{K0}}{\Omega_{m0} a_0}; \quad C = \frac{\Omega_{\Lambda 0}}{\Omega_{m0} a_0^3}; \tag{A7}$$

where we note that $B, C \ll 1$ due to $a_0 \gg 1$ and $\Omega_{m0} \sim \Omega_{K0} \sim \Omega_{\Lambda 0}$ according to the current observational results. Thus we can rewrite equation (A1) as

$$\left(\frac{da}{d\eta}\right)^2 = A^2(1 + a + Ba^2 + Ca^4); \tag{A8}$$

where

$$\eta_A = \frac{1}{\eta_{eq}} \int_0^1 \frac{da}{(1 + a + Ba^2 + Ca^4)^{1/2}} \approx A. \tag{A9}$$

Equation (A8) can then be numerically evaluated with certain choices of Ω_{m0}, $\Omega_{\Lambda 0}$ and Ω_{K0}. Assuming three species of neutrinos and using $\rho_{\gamma 0} = 2.0747 \times 10^{-51}\,\mathrm{GeV}^4$ [37] and the fact that at η_{eq} both the curvature and the cosmological constant terms are negligible in (A1), we obtain

$$a_0 = 23219\, \Omega_{m0} h^2; \tag{A10}$$

$$\eta_{eq} = 16.310\, (\Omega_{m0} h^2)^{-1}\,\mathrm{Mpc}; \tag{A11}$$

$$t_{eq} = 3.4058 \times 10^{10}\, (\Omega_{m0} h^2)^{-2}\,\mathrm{sec}; \tag{A12}$$

where η_{eq} is in the units measured today. In certain cases, (A8) can be exactly solved:

1. $K = \Lambda = 0$ (i.e. $\Omega_{m0} = 1$; $\Omega_{\Lambda 0} = 0$):

$$a(\eta) = A^2\eta^2/4 + A\eta; \tag{A13}$$

$$t(\eta) = A^2\eta^3/12 + A\eta^2/2; \tag{A14}$$

which give $\eta_{eq} = 3t_{eq}/\sqrt{2}$.

2. $K < 0$; $\Lambda = 0$ (i.e. $\Omega_{m0} < 1$; $\Omega_{\Lambda 0} = 0$):

$$a(\eta) = \frac{1}{2B}\left[\cosh(A\sqrt{B}\,\eta) + 2\sqrt{B}\sinh(A\sqrt{B}\,\eta) - 1\right]; \tag{A15}$$

$$t(\eta) = \frac{1}{AB}\left[\cosh(A\sqrt{B}\,\eta) + \frac{1}{2\sqrt{B}}\sinh(A\sqrt{B}\,\eta) - \frac{A}{2}\eta - 1\right]. \tag{A16}$$

3. $K > 0$; $\Lambda = 0$ (i.e. $\Omega_{m0} > 1$; $\Omega_{\Lambda 0} = 0$):

$$a(\eta) = \frac{1}{2B}\left[\cos(A\sqrt{-B}\,\eta) - 2\sqrt{-B}\sin(A\sqrt{-B}\,\eta) - 1\right]; \tag{A17}$$

$$t(\eta) = \frac{1}{AB}\left[\cos(A\sqrt{-B}\,\eta) + \frac{1}{2\sqrt{-B}}\sin(A\sqrt{-B}\,\eta) - \frac{A}{2}\eta - 1\right]. \tag{A18}$$

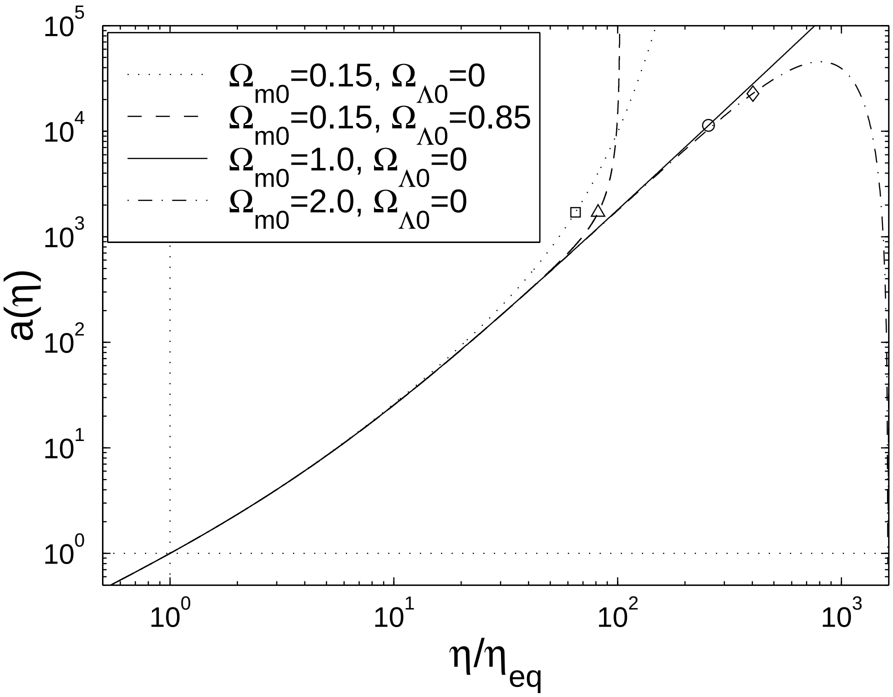

FIG. 10. The evolution of background dynamics in various cosmologies. Plotted are exact solutions of the scale factor $a(\eta)$. The square, triangle, circle and diamond mark the universe today for different models, each with $H_0 = 70$ km s^{-1}Mpc^{-1}.

We notice that at early times equations (A15–A16) and (A17–A18) reduce to equations (A13–A14). At late times equations (A13–A14), (A15–A16) and (A17–A18) give the asymptotic forms

$$a(\eta) \propto \begin{cases} \eta^2; & K = \Lambda = 0; \\ \exp(A\sqrt{B}\,\eta); & K < 0;\ \Lambda = 0; \\ 1 - \cos(A\sqrt{B}\,\eta); & K > 0;\ \Lambda = 0; \end{cases} \tag{A19}$$

or

$$a(t) \propto \begin{cases} t^{2/3}; & K = \Lambda = 0; \\ t; & K < 0;\ \Lambda = 0; \\ 1 - \cos[2A(B)^{3/2}t]; & K > 0;\ \Lambda = 0. \end{cases} \tag{A20}$$

Figure 10 shows some examples of these solutions. As we can see, the destinies of universes in different cosmologies diverge, although all have identical features around or before the radiation-matter equality t_{eq}. This converging behavior at early times helps simplify the calculation of cosmological perturbations with causal source, since we know that this kind of perturbations are mainly contributed from the radiation-matter transition era.